Broadband Two-Photon Absorption Spectroscopy: Measuring Accurate Absolute Cross-Sections

David A. Stierwalt

B.S. Chemistry, University of Indianapolis, 2016

B.S. Biology, University of Indianapolis, 2016

Submitted to the graduate degree program in Department of Chemistry and the Graduate Faculty of the University of Kansas in partial fulfillment of the requirements for the degree of Masters of Science.

Christopher G. Elles, Chairperson

Committee members

Ward H. Thompson

Carey K. Johnson

Date defended: August 15, 2019

The Thesis Committee for David A. Stierwalt certifies
that this is the approved version of the following thesis :

Broadband Two-Photon Absorption Spectroscopy: Measuring Accurate Absolute Cross-Sections

Christopher G. Elles, Chairperson

Date approved: August 15, 2019

Abstract

The properties of two-photon excitation, such as the different selection rules and superior spatial control compared with one-photon excitation, and are exploited in many different types of applications, from two-photon fluorescence microscopy to photodynamic therapy. Most prior work has emphasized the development of molecules with large two-photon absorption (2PA) cross-sections using single wavelength measurements that neglect the rich information available from broadband 2PA spectroscopy. Techniques that have been used to measure two-photon absorption spectra are often complicated by large experimental uncertainties. This thesis describes work to develop a broadband two-photon absorption method in order to provide a robust method that can accurately measure two-photon absorption spectra and absolute cross-sections, and therefore aid in the discovery of novel chromophores with large two-photon cross-sections for use in many different applications.

The work presented in this thesis involves method development of the broadband two-photon absorption technique through measurements of the test compounds coumarin 153 and benzene. The broadband two-photon absorption technique simultaneously measures stimulated Raman scattering that can be used as an internal standard in the measurement of absolute two-photon absorption cross-sections. In addition, picosecond pump pulses were used in the broadband two-photon absorption method to increase the resolution of the technique. Lastly, improvements to the broadband two-photon absorption technique were used in a preliminary study of photo-active manganese tricarbonyl complexes to demonstrate how two-photon absorption spectroscopy is helpful for understanding the non-linear photo-induced release of carbon monoxide.

Acknowledgements

First I would like to thank my advisor Chris Elles for his patience and mentorship throughout the last three years as I have developed both as a researcher and scientist. His constant enthusiasm for my research has constantly inspired me through the rough patches and has helped to push my research forward in order to obtain my goals. I am immensely thankful for all the time Chris has spent over the last three years teaching me new techniques and introducing me to the field of ultrafast laser spectroscopy. In addition, Chris has provided wonderful opportunities for me to present my research to other researchers in my field and provided opportunities to personally meet excellent scientists along the way. Lastly, I am thankful for his constant consideration for both my time at the University of Kansas and for the future.

Secondly I would like to thank all of the members of the Elles Research Group: Dr. Tim Quincy, Dr. Chris Otolski, Kristen Burns, Pransenjit Srivastava, Dan Johnson, Emmaline Lorenzo, Sadegh Mahvidi, Brooks Hidaka and Whitney Harmon for the constant support and encouragement. All of who have contributed to this work through constant scientific discussion about my research and support when research did not go as planned. I would also like to specifically thank Dr. James Blakemore and Wade Henke for the wonderful collaboration with manganese carbonyl complexes project.

Next, I would like to thank my new friends from the University of Kansas and old for the constant support and encouragement that has been crucial to my success these three years. I would also like to thank my family for understanding and allowing me to prioritize my research and education for whom moving to Kansas would have been impossible without. Lastly, but certainly not least, I would like to thank my amazing wife Lizzie for her unending support and compassion throughout my time at the University of Kansas and without her this work would not have been possible, and Rock Chalk.

Contents

List of Figures

List of Tables

Chapter 1

Introduction

1.1 Overview of Two-Photon Absorption

Research over the past two decades has led to the development of molecules that readily undergo two-photon absorption (2PA), i.e. molecules with large 2PA cross-sections.[1,2] A few of the applications that take advantage of the properties of nonlinear absorption are two-photon fluorescence microscopy,[3–13] photodynamic therapy (PDT),[14–27] and optical data storage.[28] For the continued development of these many promising applications, new two-photon chromophores with large absolute 2PA cross-sections are required. However the ability to measure the broadband two-photon absorption spectra and absolute cross-sections is limited by the current techniques available which all have large experimental uncertainties and require ultrafast laser pulses to generate the required intensity to initiate two-photon absorption.[29] The work in this thesis develops and improves the ability of the broadband two-photon absorption technique to measure accurate two-photon absorption cross-sections and broadband spectra to aid in the research of novel two-photon chromophores.

Two-photon absorption spectroscopy is a powerful technique that is critical in understanding the electronic structure of molecules. Two-photon absorption spectroscopy can probe the different two-photon allowed electronic states and how readily a molecule will undergo two-photon absorption by measuring the absolute two-photon absorption cross-section. Two-photon absorption spectroscopy can be used in combination with many different wavelength photons and different polarizations to interrogate the electronic excited states of a molecule. To better understand the relationship between the structure of molecules and their two-photon absorption properties accurate broadband 2PA spectroscopy is required. Therefore the development of the broadband 2PA

technique is key in the further development of novel 2PA chromophores designed for use in the applications using two-photon excitation.

The many advantages of two-photon absorption are derived from the fact that two-photon absorption can be induced using two non-resonant photons. Two-photon absorption can be achieved using either a single laser source or by using two different laser sources and different wavelength photons. The simultaneous absorption of two-photons of the same wavelength is shown in Figure 1.1. The combined energy of the two non-resonant photons can promote a molecule to an excited state but only through the simultaneous absorption of both photons.[29]

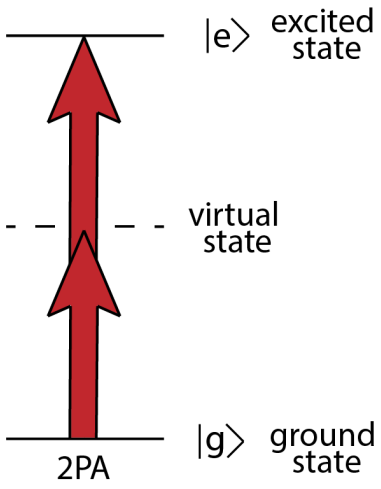

Figure 1.1: Energy level diagram of two-photon absorption including the virtual state

The non-resonant photons require that two-photon absorption proceeds through a virtual state shown in Figure 1.1. The virtual state is described as the perturbed molecule in the presence of the incident electric field. Therefore, when overlapped with a second field 2PA can achieve promotion to an allowed electronic excited state, as shown in Figure 1.1. Two-photon absorption cross-sections can be described using the sum over states to describe the electronic dipole contributions to the two-photon transition.

$$\sigma_{2PA} \propto \sum_i \left[\frac{\langle g|\mu \cdot \varepsilon_{pump}|i\rangle \langle i|\mu \cdot \varepsilon_{probe}|e\rangle}{\hbar\omega_{pump} - E_{ig}} + \frac{\langle g|\mu \cdot \varepsilon_{probe}|i\rangle \langle i|\mu \cdot \varepsilon_{pump}|e\rangle}{\hbar\omega_{probe} - E_{ig}} \right]^2 \tag{1.1}$$

Here the two terms within the sum represent the different ordering of the interactions where both terms correspond to reaching the same excited electronic state e. The components in the numerator of equation 1.1 are the dipole operator μ, polarization vectors of each electric field ε_{pump} and ε_{probe}, and the corresponding wavefunctions for the different states g, e, and i. The terms in the numerator describe the two-photon absorption process where the first perturbation ε_{pump} is promoting the system through the interaction with the electronic dipole μ from the ground electronic state g to the intermediate state i and then the second perturbation ε_{probe} promotes the system to the final electronic excited state e. Lastly, the denominator represents the difference in energy between the photons involved and the eigenstates of the system. The individual terms increase as the energy separation between the photon and the eigenstates becomes small and therefore, are moving on resonance with that transition.

The coupling of two electronic transition dipoles is what leads to the difference in the selection rules for two-photon absorption compared to traditional one-photon absorption, and makes two-photon absorption an important spectroscopic tool. The allowed electronic transitions for both one and two-photon absorption are determined by the molecular symmetry of the molecule and the character tables for each corresponding point group.[30–32] Molecules are sorted into different point groups based upon the symmetry operations that are present in each molecule. The main and most notable difference in the selection rules for two-photon absorptions arises from molecules which are classified as centrosymmetric meaning that they contain a center of inversion. The parity selection rules for centrosymmetric molecules for one-photon absorption transitions requires a change in the inversion symmetry of the electronic state. The inversion symmetry of the orbitals is described as *gerade*(symmetric) or *ungerade*(antisymmetric). Therefore the parity selection rules for one-photon transitions in centrosymmetric molecules require either a transition from a symmetric(g) to an antisymmetric(u) state or vice versa. The parity selection rules for two-photon absorption for centrosymmetric molecules are notably different due to the two interactions with the electric fields (pump and probe). The parity selection rules for two-photon absorption do not allow a change in the inversion symmetry between the initial and final electronic states, therefore

allowing transitions from symmetric(g) ground states to symmetric excited states(g) and the same applies from antisymmetric states. Therefore, granting access to different excited electronic states after two-photon absorption for centrosymmetric molecules. Lastly, the parity selection rules for non-centrosymmetric molecules are not exclusive between one and two-photon absorption and therefore the allowed transitions are determined by the symmetry of the molecule.

Access to different electronic states through different selections rules has inspired research to control and better understand the photo-chemical reactions through one and two-photon processes.[33–35] Photo-chemical reactions are controlled by the landscape of the excited state potential energy surface and therefore can achieve different results based upon the excitation source either by one or two-photon absorption. This has directly motivated previous research in our group looking at the two-photon un-caging reactions in a *p*-hydroxyphenacyl for controlled release of ATP and understanding how the photoisomerization of trans-stilbene is affected by higher-lying excited states[27,36]. Being able to thoroughly investigate the two-photon absorption properties of molecules is imperative to the continued development of novel two-photon active materials and the advancement of this field of research.

1.2 Applications of Two-Photon Absorption

The properties of two-photon absorption have been demonstrated to be useful in many different applications from photodynamic therapy to two-photon fluorescence microscopy.[3,20] The properties of two-photon absorption are described by the change of intensity of a laser beam that is transmitted through a sample in the z-direction, as shown by equation 1.2. The first term shows the one-photon absorption is linearly related to the change in intensity as the beam is transmitted, and the two-photon absorption is quadratically related. The terms α and β are related to the one and two-photon absorption cross-sections, and the relationship between the two-photon coefficient and the two-photon absorption cross-section is shown in Equation 1.3. Therefore, only when the laser beam is non-resonant and one-photon absorption is weak can two-photon absorption compete to

attenuate the transmitted laser beam.

$$\frac{\partial I}{\partial z} = -\alpha I - \beta I^2 \tag{1.2}$$

$$\beta = \frac{n}{\hbar\omega}\sigma_{2PA} \tag{1.3}$$

The two-photon absorption cross-section is usually given in the units of Goppert-Mayer (GM) where 1 GM is equal to $10^{-50}(\frac{cm^4 * s}{molecule * photon})$. For appreciable two-photon absorption to occur large intensities are required and can be achieved by the use of ultrafast pulsed laser sources. The intensity dependence is one reason two-photon absorption has been used in many applications such as two-photon florescence imaging and photodynamic therapy.

1.2.1 Two-photon Fluorescence Imaging

A main application for two-photon absorption is two-photon microscopy which was first demonstrated in 1990 by Denk *et al.*[3] with two-photon laser scanning microscopy. Two-photon microscopy since then has developed into many other techniques based on the properties of two-photon absorption such as multiphoton microscopy and deep two-photon microscopy however each technique intentionally takes advantage of the properties of nonlinear absorption.[6,10] The spatial control of two-photon absorption granted from the intensity dependence allows for the ability to reduce out of focus excitation by only selectively exciting molecules within the intense laser focus. In addition, two-photon absorption can excite visible or ultra-violet transitions using near-IR photons because it is the combined total energy of both photons that determines which electronic transition is excited. The use of longer wavelength near-IR photons that are known to better penetrate highly scattering tissues such as the skin allows for deep imaging using nonlinear absorption.[7,10] Two-photon fluorescence imaging has been widely implemented.[3–8,37] Due to the successful application of two-photon microscopy, a large number of two-photon molecular fluorescent probes have been developed for a wide range of imaging applications.[11,38–41] The development of these probes is dependent upon their two-photon absorbing properties and the techniques available to measure

them. Therefore the development of a simple and accurate method for measuring two-photon absorption spectra such as the broadband two-photon absorption technique can directly lead to the development of novel nonlinear fluorescent probes.

1.2.2 Controlling Chemical Reactions with Two-Photon Absorption

An important goal in almost every area of chemistry research is to better understand chemical reactions to develop ways to exert control over the outcome of reactions.[42] The properties of two-photon absorption have been often employed to help control chemical reactions by accessing different electronic states through two-photon absorption processes. The previously described selection rules allow for molecules which are centrosymmetric to reach different electronic states and thus possibly allowing for different excited state dynamics that could help lead to controlling photochemical reactions. One example of this approach was used by Sotome *et al.* to increase the quantum yield of the cycloreversion reaction of a diarylethene photoswitch for possible applications in optical data storage.[43] For photochemical reactions, the electronic states involved playing a critical role in determining the reactivity. For the condensed phase, Kasha's rule states that higher lying excited states are rapidly relaxed through internal conversion to the lowest-lying excited state generally, the S_1 state which limits the ability for higher-lying excited states to control chemical reactions.[44]

Controlling chemical reactions using two-photon absorption can often be limited by both Kasha's rule and molecules that are not centrosymmetric.[44] Low-symmetry molecules typically reach similar electronic excited states with both one and two photon absorption. However, the use of two-photon absorption for applications in photodynamic therapy can still take advantage of the other properties of two-photon absorption. The superior spatial control and lower energy photons involved help to motivate additional applications such as photodynamic therapy and two-photon fluorescence imaging to take advantage of two-photon absorption. Two-photon absorption has been demonstrated for many different types of photodynamic therapies including the production of singlet oxygen species for anti-cancer or apoptotic behavior.[16,22,45–47] Also, there are many

other examples of the use of two-photon excitation to control photochemical reactions. Another example includes the photo-uncaging for controlled release of adenosine triphosphate (ATP) and other neurotransmitters previously studied within our group.[36]

1.3 Two-photon Absorption Techniques

1.3.1 Degenerate 2PA Spectroscopy Methods

1.3.1.1 Z-scan

The most common technique for two-photon absorption spectroscopy and nonlinear absorption measurements is the z-scan technique.[48–50] The z-scan technique uses a single pulsed monochromatic beam. The beam is focused tightly to produce the sufficient intensities to generate the desired two-photon absorption, and the sample is translated along the axis of the beam denoted the z-axis. The z-scan technique directly measures the transmission and therefore, the attenuation of the laser beam at the specific position along the z-axis due to two-photon absorption. The incident laser energy per pulse is kept constant throughout the measurement; however, the intensities are changed due to the focusing of the beam and the translation of the sample through this focus. An additional benefit is that the z-scan has also been demonstrated to simultaneously measure the nonlinear refraction and the two-photon absorption in closed aperture configuration, while also being able to unambiguously separate both signals.[49] The versatility and simplicity of the technique is the reason why it is a very common method used for nonlinear absorption studies. The largest drawback of the traditional single beam z-scan measurement is that to measure broad spectral dependence requires several z-scan measurements and tuning of the laser wavelength.

A variation of the z-scan technique was demonstrated using femtosecond white light continuum instead of the traditional single monochromatic beam.[51] The white light continuum z-scan greatly simplified the measurement of the broad spectral dependence. This enabled the measurement of the broadband two-photon absorption spectrum without the need for tuning the laser wavelength

and multiple measurements. The complications to this technique come from generating enough intensity in the white light continuum for two-photon absorption to take place. The white light continuum z-scan measurements by De Boni *et al.* required approximately $10\mu J$ per pulse of white light continuum in their measurements compared with only a few *nJ* in typlical WLC probe pulses.[52] While generating large amounts of white light continuum, great care needs to be taken in order to measure the spatial dependence of the focus of the broadband white light continuum in order to ensure the white light is composed of a singular beam and not composed of multiple filaments. The white light continuum z-scan is a unique capability of the z-scan technique, however the monochromatic z-scan is the predominantly used technique. The implementation of white light continuum z-scan highlights the difficulty of measuring the broadband two-photon absorption spectrum and the need for the continued development of the current methods used to measure two-photon absorption.

1.3.1.2 Two-Photon Induced Fluorescence

Another two-photon absorption technique that has been demonstrated is the two-photon excitation fluorescence technique as shown in the work by Xu *et al.*[53] This technique is characterized by measuring the fluorescence signal that is produced after a degenerate two-photon excitation. Therefore, it is not directly measuring the absorption by the way of the attenuation of the transmitted beam like the z-scan technique but instead, the fluorescence signal is measured. Therefore this technique is relying on the two-photon fluorescence quantum yield being directly proportional to the absolute two-photon absorption cross-section and that the molecule of interest is fluorescent. This degenerate two-photon absorption technique again is limited by the tuning of the laser wavelength to capture the entire two-photon absorption spectrum.

This technique is notably used by De Reguardati et al. for some of the most accurate measurements of absolute two-photon absorption cross-sections of common fluorescent laser dyes to be used as reference standards for nonlinear absorption.[54,55] Their results are used as a point of

comparison for the work in this thesis. The two-photon induced fluorescence technique has been used to measure multiple series of reference standards and most notably include the work done by both Xu and DeReguardati *et al.*[53,54] Ultimately all the methods used to measure two-photon absorption cross-sections are complicated by the necessity of ultrafast laser pulses which can lead to large systematic uncertainties. The uncertainties arise from the necessity of knowing the full 3-D intensity profile of the ultrafast pulse where hot spots or deviations from Gaussian character can lead to large uncertainties. However, some of the most common applications for two-photon absorption are the two-photon fluorescence microscopy and the development of nonlinear fluorescent probes. Therefore the fluorescent references standards are often used to help measure and ensure the two-photon fluorescence properties of novel fluorescent probes making this the technique that is most commonly used for molecules of this type. There have also been series of reference standards measured for other types of materials based on their applications.[53–57]

1.3.2 Non-Degenerate 2PA Spectroscopy Methods

The simultaneous absorption of two photons of different wavelengths is non-degenerate two-photon absorption and requires two different ultrafast laser pulses overlapped in time and space within the sample. The introduction of a second beam complicates the technique from a technical standpoint, but as demonstrated in the work for this thesis and by others[58–60], the additional laser pulse opens up opportunities for improving the techniques for two-photon absorption spectroscopy. Most notably was the use of the ultrafast white light continuum in addition to an intense pump pulse to achieve broadband detection in a single measurement. Another benefit of two-beam techniques is that the polarization dependence can be easily measured by rotating the polarization of a single beam relative to the other. The introduction of two laser pulses is greatly beneficial to the overall method development of two-photon absorption spectroscopy.

The broadband two-photon absorption technique is a pump-probe derived technique that is analogous to traditional transient absorption spectroscopy, but instead of looking for the dynamical

information, the absorption of the probe in the presence of a non-resonant pump pulse is measured. This technique was first demonstrated in the work done by Negres *et al.* in 2002.[58,59]Broadband two-photon absorption uses a weak ultrafast white light continuum often denoted as the "probe" pulse for broadband detection and an intense ultrafast "pump" to achieve the intensity and photon flux needed for two-photon absorption. This technique has been demonstrated to be a powerful tool to probe the electronic structure of water and common alcohols in the ultraviolet region using the polarization dependence in the work done by Elles *et al.*[60] and Bhattacharyya *et al.*[61] The ability to resolve solvation effects in green fluorescent protein (GFP) was also demonstrated in the work done by Hosoi *et al.*[62]

1.4 Thesis

This thesis discusses the development of the broadband two-photon absorption spectroscopy technique by the implementation of stimulated Raman scattering as an internal standard to reduce the experimental uncertainty in the measurement of the absolute 2PA cross-section and the incorporation of picosecond pump pulse to improve the resolution of the technique. The development is intended to simplify the measurement of absolute two-photon absorption cross-sections and the measurement of accurate two-photon absorption spectra.

The second chapter of this thesis discusses the experimental methods of the broadband two-photon absorption and polarization gated frequency-resolved optical gating (PG-FROG) techniques. The broadband two-photon absorption technique used multiple detection schemes and pump pulses. The ps pump pulses were generated using second-harmonic spectral compression and filtered using a 4f filter in order to produce narrow bandwidth Gaussian ps pulses for broadband 2PA measurements. The different detection schemes were used to increase the experimental resolution for the broadband 2PA measurements. The PG-FROG setup was implemented for diagnostic purposes to measure the spectrogram of the fundamental output of a Ti:Sapphire (Coherent, Legend Elite) laser.

The third chapter describes the method development of the broadband two-photon absorption technique. The broadband two-photon absorption spectrum of coumarin 153 was measured to demonstrate the overlapping stimulated Raman scattering and two-photon absorption signals that can be used as an internal standard. The internal standard was demonstrated to eliminate the uncertainty in the overlap of the pump and probe which is the largest source of experimental uncertainty in the measurement of the absolute two-photon absorption cross-section using the broadband 2PA technique.

The work in the fourth chapter of this thesis describes the incorporation of a spectrally filtered ps pump pulse for the broadband two-photon absorption technique. The ps pump pulse was used to measure the two-photon absorption spectrum of the electronically forbidden $B_{2u} \leftarrow A_{1g}$ transition of benzene. The known one-photon and two-photon absorption spectroscopy of benzene enable the assignment of the vibronic progressions measured using the broadband two-photon absorption technique. The picosecond pump pulse was used to test the resolution of the technique and to show the natural linewidth of the vibronic bands in condensed phase benzene. The incorporation of the picosecond pump pulses improves the use of the stimulated Raman scattering as an internal standard by improving the ability to resolve the individual Raman bands and increase the accuracy of differential Raman cross-section.

The last chapter of this thesis describes how this research for both the method development and two-photon absorption spectroscopy can be continued in the future. The preliminary study of a class of manganese tricarbonyl complexes which have demonstrated the photo-induced release of carbon monoxide shows how the broadband two-photon absorption technique can be used to understand the two-photon electronic transitions in molecules. To demonstrate how understanding the two-photon absorption transitions can be used to maximize the two-photon absorption cross-section while maintaining the desired carbon monoxide release. Secondly, the broadband two-photon absorption can be improved by developing a single-shot measurement. In a similar manner single-shot PG-FROG can measure both the time and frequency domains of an ultrafast laser pulse in a single shot. The simultaneous measurement of both the time and frequency domains in the

PG-FROG measurement can be used to demonstrate the idea of a single-shot two-photon absorption measurement. The elimination of the use of optical delay stages and using a similar strategy to that implemented in the PG-FROG measurement, the broadband technique is a promising method for collecting single-shot broadband two-photon absorption spectra.

Chapter 2

Experimental Methods

2.1 Overview

This chapter focuses on the technical aspects of the various experimental configurations used in the development of broadband two-photon absorption measurements. The broadband two-photon absorption technique was implemented with both a femtosecond and picosecond pump pulse and two different detection methods. The different pump pulses and detection methods were used to test and improve the experimental resolution of the condensed phase broadband two-photon absorption measurements. In addition, polarization gated frequency-resolved optical gating (PG-FROG) was implemented to take single-shot measurements of the spectrogram of ultrafast laser pulses for diagnostics purposes, as demonstrated by Trebino *et al.*[63,64] The spectrogram includes the simultaneous measurement of both the time and frequency domains of an ultrafast laser pulse.

2.2 Broadband Two-Photon Absorption Setup

The broadband two-photon absorption technique required two laser beams and is directly related to the common pump-probe spectroscopy.[58,59] In a pump-probe measurement, the pump beam is generally narrow in bandwidth and typically tuned to a ground state electronic resonance of the sample to promote population to an excited state. However, in the broadband two-photon absorption, the pump beam is specifically tuned to be non-resonant with any electronic resonances and instead chosen to give the desired total energy between the pump and probe photons. The probe

beam is the same in both pump-probe and broadband two-photon absorption consisting of a weak broadband white light continuum which is also non-resonant. Therefore, the combined energy of the pump and probe photons determines the range of the two-photon absorption spectrum that is measured.

The broadband two-photon absorption measurements were taken using a Ti:sapphire oscillator (Coherent, Mantis) and amplifier (Coherent, Legend Elite) which produce 800 nm pulse with a duration of 35 fs and at a 1 kHz repetition rate. The tunable narrowband pump wavelengths were generated using a commercial optical parametric amplifier (OPA) with two additional frequency conversion stages. The probe white light continuum was produced by the use of a home built OPA whose infrared 1200 nm signal pulse was focused into a circularly translating CaF_2 disc to produce the desired wavelength range of the continuum.[35] Overlapping the pump and probe in time was achieved with optical delay stages. The pump and probe are tightly collimated around 150 μm beam diameter and overlapped spatially within the sample 1 cm cuvette.

The two-photon absorption spectrum is calculated using the difference absorption signal (ΔA) and is measured using alternating measurements of the probe intensity when the pump is incident (I_{on}) and when the pump is blocked (I_{off}).

$$\Delta A = -log_{10}(\frac{I_{on}}{I_{off}}) \tag{2.1}$$

Synchronized optical choppers (Newfocus,3501) set to 500 Hz block every other pump pulse to facilitate shot to shot measurement of the change in absorption during broadband two-photon absorption measurements.

2.2.1 Picosecond Pump Pulse Generation

The broadband two-photon absorption measurements that included the simultaneous measurement of stimulated Raman scattering are discussed in further detail in chapter 3 of this thesis. The use of a femtosecond pump pulse with considerable bandwidth limits the ability of the technique to

resolve narrow Raman scattering peaks. The use of picosecond pump pulses for stimulated Raman scattering measurements has been documented previously.[65] The use of narrow-bandwidth picosecond pump pulses ensures that the pulse duration is larger than vibrational decoherence time of the stimulated Raman signal to eliminate any artifacts in the Raman signals. Also, the narrow bandwidth of the picosecond pump pulse ensures that there is limited broadening of the natural linewidth of the Raman peak which arises from dephasing lifetime of the vibration.[66] Therefore, the combination of the picosecond pump pulses and the broadband two-photon absorption technique improved the ability to resolve narrow Raman bands.

The picosecond pump pulses were generated using second harmonic spectral compression and spectrally filtered using a 4f filter as demonstrated by Pontecorvo *et al.*[67] The wavelength pump pulse is specifically chosen in order to produce the desired pump wavelength after the second harmonic generation occurs. The second harmonic generation takes place in a long β-barium borate (BBO) crystal to produce a stretched pulse at twice the incident frequency. The length of the BBO and the index of refraction of the second harmonic pulse leads to an asymmetric pulse shape that can lead to artifacts in the stimulated Raman signals. The use of a 4f spectral filter is used to produce narrow bandwidth Gaussian-shaped pulses.[65–67]

2.2.2 Detection Methods

The detection methods for the broadband two-photon absorption measurements varies between the experiments with the picosecond and femtosecond pump pulses. Different detection methods were tested to increase and test the resolution of the broadband two-photon absorption measurements. The femtosecond pump pulse experiments used a 300 lines/mm transmission grating and a 256-pixel silicon photodiode array (Hamamatsu, S3901-256Q) for the white light to be dispersed. This setup was limited by the amount of white light that could be dispersed across the limited number of pixels. In order to increase the resolution of the broadband two-photon absorption, the use of a 1/8 m imaging spectrograph and a linear charge-coupled device (CCD) (Hamamatsu, S11156-2048)

detector with 2068 pixels was used. The spectrograph has multiple entrance slits and gratings to achieve the desired resolution and is described in further detail in the dissertation of Timothy Quincy and chapter 4 of this thesis.[66]

2.3 Polarization Gated Frequency Resolved Optical Gating (PG-FROG)

The complete characterization of an ultrafast laser pulse was obtained from a PG-FROG measurement.[63,64] The PG-FROG setup is shown in the schematic diagram in Figure 2.1. The fundamental output of the Ti:Sapphire laser is split into two beams, the pump and probe, and overlapped within a fused silica medium by the use of a delay stage. The polarization of the pump beam, which is

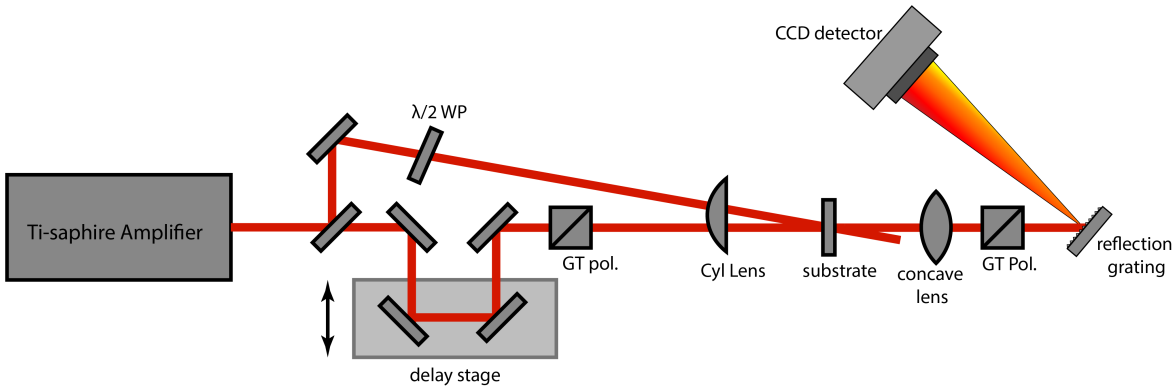

Figure 2.1: Schematic diagram of PG-FROG setup

not collected or dispersed onto the detector, is rotated by 45 degrees using a half-wave plate. Both the pump and probe beams are focused to a line using a cylindrical lens with a focal distance of 75 mm to encode the temporal information. The line focus of both the pump and probe means that spatially when the two beams are crossed at a small angle the overlap encodes the temporal domain in the spatial beam profile. The fused silica substrate is placed within the overlapping foci of the pump and probe beams. The probe beam is then passed onto a Glan-Thompson polarizer set perpendicular to the probe polarization. This polarizer blocks almost all of the incident light from reaching the detector which is a 2-D pixel array CCD camera.

The PG-FROG measurement is a powerfully simple technique that can measure both time and frequency domains of an ultrafast laser pulse in a single-shot. The PG-FROG technique works by

using the pump beam to induce the optical Kerr effect to rotate the polarization and to gate the interaction between pump and the probe pulse. The measured signal arises from the electric fields that have had their polarization shifted by the optical Kerr effect and the interaction with the pump when overlapped within the fused silica medium. Therefore the polarizations of the electric fields that have been rotated due to the optical Kerr effect are able to pass through the perpedicular polarizer and be dispersed onto the CCD camera. Therefore allowing for the measurement of the time and frequency domains of ultrafast laser pulses. The single-shot nature of the FROG techniques make it a powerful diagnostic tool for ultrafast laser research that can be used to measure the group velocity dispersion of ultrafast laser pulses without the need for signal processing.

Chapter 3

Measurement of Broadband Two-Photon Absorption Spectra and Accurate Absolute Cross-sections of Coumarin 153

3.1 Introduction

Two-photon excitation plays an essential role in many applications, including two-photon fluorescence imaging,[3–8,13] photodynamic therapy (PDT),[14–16,18–20] and 3D data storage.[28] Although demonstrated almost sixty years ago, non-linear absorption has many unique properties that make it an important part of many applications, even today.[68] A characteristic property of two-photon absorption is that it requires a high-intensity light source on the order of gigawatts per square centimeters ($10^9 \frac{W}{cm^2}$) in order to achieve two-photon absorption. Another benefit in the applications of fluorescence microscopy is that the high intensities eliminates the out of focus absorption where the intensity is not large enough to induce two photon absorption. This leads to a highly controlled excitation volume.[8] Lastly, 2PA requires lower energy photons for excitation because it is the combined total energy of the two photons being absorbed. Therefore, near-IR photons can be used in many applications which can better penetrate highly scattering tissues and can replace potentially harmful visible or even UV photons.[3,15]

The useful properties of two-photon absorption and the many applications that use it have inspired a great deal of work in the development of novel two-photon chromophores with large 2PA cross-sections for use in these applications. The development of new two-photon chromophores is limited by the single wavelength techniques available to measure the 2PA spectra and the significant uncertainty in the absolute 2PA cross-sections. The problematic nature of measuring the 2PA

spectra and absolute 2PA cross-sections is directly related to the considerable uncertainty associated with knowing the full 3-D intensity profile of a laser pulse. Therefore, since all techniques to measure the absolute 2PA cross-section require the use of intense laser pulses, and therefore all carry significant experimental uncertainties.

The most commonly implemented technique is the z-scan in which the sample is translated through a focused laser along the z-axis. Therefore, the transmitted laser intensity is directly measured at each z-axis position to measure the attenuation from two-photon absorption.[49,69] There are multiple configurations of the z-scan technique, including the open and closed aperture. The open-aperture case can be used to measure two-photon absorption, and the closed-aperture configuration measures the non-linear refractive index.[70] The other commonly used technique is the two-photon excitation fluorescence (2PEF) method. This technique does not directly measure the absorption. However, it measures the induced fluorescence signal from two-photon absorption. The measurement of the 2PA cross-section from the fluorescence signal was shown by Hermann et al.[71] where the absolute 2PA cross-section can be calculated for a system if the fluorescence quantum yield and the laser flux distribution are well known and by measuring the resulting fluorescence intensity.

The major drawback of both the monochromatic z-scan and 2PEF techniques is obtaining the broadband 2PA spectrum requires tuning across many different wavelengths. A z-scan technique that can measure the continuous 2PA spectrum using high-intensity broadband continuum has been demonstrated to eliminate this disadvantage.[52,72,73] Another technique that can measure the broadband 2PA spectrum without the tuning of the laser wavelengths is the broadband 2PA technique. The broadband 2PA technique combines a femtosecond white light continuum probe and an intense pump beam to measure the 2PA spectra by directly measuring the attenuation of the probe photons.[58,59] The broadband continuum probe allows for the measurement of the continuous 2PA spectrum and eliminates the necessity for single-point measurements commonly used in z-scan and two-photon fluorescence methods. The broadband two-photon absorption technique is closely related to pump-probe spectroscopy, except that the pump wavelength is non-resonant with the

electronic transitions of the molecule. The pump wavelength is chosen in consideration of the combined total energy of the pump and probe that gives the desired region of the 2PA spectrum.

The primary source of uncertainty for the measurement of the absolute 2PA cross-section is knowing the full three-dimensional intensity profile of an ultrafast laser pulse. Any irregularity in the shape or hot spots in the ultrafast laser pulses can lead to systematic errors and large uncertainties. In addition, to measure the two-photon absorption spectrum using the z-scan or 2PEF techniques the tuning of the laser wavelength is required. This tuning of the laser can also introduce subtle variations from wavelength to wavelength in the intensity profiles leading to additional error when measuring the absolute 2PA cross-sections across a series of laser wavelengths. Regardless of the technique, all 2PA measurements are susceptible to systematic errors from the intensity profiles of the laser pulses involved. There has been considerable work to accurately measure series of 2PA reference standards for multiple classes of molecules to help reduce the overall uncertainty in measurements of the absolute 2PA cross-sections.[54–56,74]

In this work, we take advantage of stimulated Raman scattering signals as an internal standard for the measurement of absolute 2PA cross-sections. Both stimulated Raman scattering (SRS) and 2PA are nonlinear processes that can be measured simultaneously using the broadband 2PA technique. The simultaneous measurement was demonstrated by Isobe et al. using both 2PA and SRS signals for nonlinear microscopy.[75] Using the broadband 2PA technique, we use the simultaneous measurement of both 2PA and the SRS as an internal standard to calculate accurate absolute cross-sections independent of overlap as well as measuring broadband continuous 2PA spectra.

3.2 Methods

The broadband 2PA method is a pump-probe measurement that has been described previously.[58,59,76] Two separate laser pulses are overlapped both spatially and temporally within the sample. The pump pulse in the broadband 2PA measurement is chosen to be non-resonant with any allowed electronic transitions in the sample. The weak probe pulse is a broadband white-light continuum (WLC) covering the visible region of the spectrum, as shown in Figure 3.1. Using the WLC in

broadband 2PA spectroscopy serves the same purpose as in traditional pump-probe spectroscopy, which allows for the measurement of the broad spectral dependence in a single measurement. Also, shown in Figure 3.1 is stimulated Raman scattering (SRS) which has the same experimental requirements of a non-resonant pump and WLC probe as the broadband 2PA measurement, and therefore both signals can be measured simultaneously.

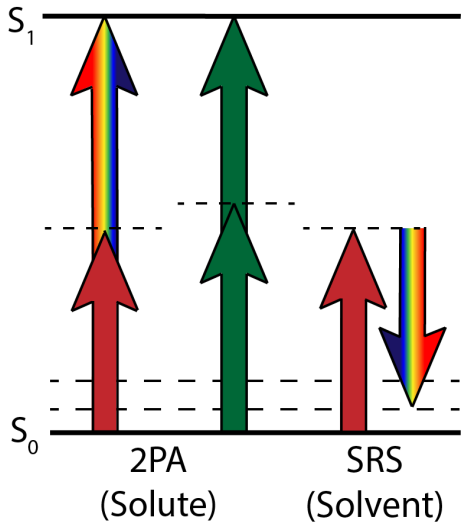

Figure 3.1: Energy level diagram showing degenerate and non-degenerate two-photon absorption of the solute and stimulated Raman scattering processes in the solvent.

The region of the 2PA spectrum that is measured is defined by the combined total energy of the pump and broadband probe photons. The location of the SRS is determined by the pump wavelength and the frequency of the observed Raman bands. The broadband 2PA technique measures the direct attenuation of the probe pulse in the presence of the pump; therefore, directly measuring the 2PA and SRS signals across all combinations of pump and probe photons. Due to the group velocity delay (GVD), the different wavelengths of the WLC arrive at the sample at varying times. Therefore, the pump-probe delay must be scanned to ensure that all wavelengths of the WLC interact with the pump pulse within the sample. The direct 2PA and SRS spectrum of the sample can be measured across a broad range of total energy using the broadband 2PA method.

The absolute 2PA cross-section describes the sample's ability to attenuate light via a 2PA process and is directly related to measuring the 2PA spectrum of the sample. The absolute two-photon

cross-section as a function of energy is proportional to the time-integrated absorption signal at each probe wavelength, where E_{pump} is the pump energy per pulse in (J), l the path length of the sample, ω_{pump} the angular frequency of the pump photons in (radians/s), N_{solute} the number density of the solute in (molecules/cm^3), and GF the intensity weighted overlap between the pump and probe pulses in (cm^{-2}).

$$\sigma_{2pa}(E_{total}) = \frac{1}{GF}\frac{ln(10)}{E_{pump}l}\frac{\hbar\omega_{pump}}{N_{solute}}\int \Delta A_{2PA}(\tau)d\tau \tag{3.1}$$

Knowing the overlap between the pump and probe is critical for the calculation of the absolute 2PA cross-section from the pump-probe signal. The estimation of the pump-probe overlap is the most significant source of uncertainty in the broadband 2PA measurement. The overlap factor (GF) is used to account for the overlap between the pump and probe and is estimated by the relative spot size of the pump and probe pulses.

$$GF = \frac{1}{\sqrt{(2\pi[(\omega_x^{pr})^2 + (\omega_x^{pu})^2])}}\frac{1}{\sqrt{(2\pi[(\omega_y^{pr})^2 + (\omega_y^{pu})^2])}} \tag{3.2}$$

By measuring the beam diameters from both pump and probe in the x and y dimension, ω_x or ω_y, the overlap can be estimated. The overlap factor assumes that the pump and probe beams are collinearly propagating and that the pulses are collimated over a short distance and represented by a 2D Gaussian-shaped intensity profile. In Figure 3.2, the overlap of the pump and probe is shown where the darkened region represents the possible area where simultaneous absorption of the pump and probe can occur. The broadband 2PA technique used in this work has the two beams crossed at a small angle as diagrammed in Figure 3.2. Maximizing the overlap between the pump and probe beams during the experiments gives the largest absorption signal and most accurately matches the estimations made in the overlap factor.

Stimulated Raman scattering and broadband 2PA measurements both use a pump and broadband probe overlapped spatially and temporally. The simultaneous measurement of both 2PA and SRS will ensure that both signals are dependent on the same experimental conditions, such as the

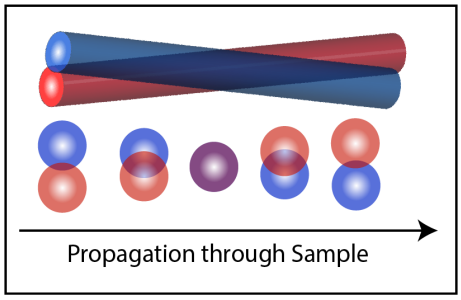

Figure 3.2: The crossing angle and overlap between the pump and probe pulses are shown along with cross-sections of the overlap along the propagation axis. The darkened purple areas where the pump and probe pulses are overlapped represent the regions where 2PA is occurring

overlap of the pump and probe. The SRS signals come predominately from the solvent due to the higher number density of solvent molecules compared to the solute. The differential Raman scattering cross-section is proportional to the time and frequency integrated Raman scattering peak from the solvent.

$$\frac{d\sigma_{Raman}}{d\Omega} = \frac{1}{GF}\frac{ln(10)}{E_{pump}l}\frac{\hbar\omega_{pump}}{8\pi^3c^2}\frac{\omega_{probe}^2}{N_{solvent}}\int\int \Delta A(\tau,\omega)d\tau_{2PA}d\omega_{Raman} \tag{3.3}$$

Where Ω is the solid angle, ω_{pump} is the angular frequency of the pump photons in (rads/s), and ω_{probe} is the angular frequency of the scattered photons. The solid angle Ω is the angle at which the photon is reflected after undergoing Raman scattering. In stimulated Raman scattering, there is no angular dependence of the scattering event because the SRS signal is phase-matched to the probe pulse.[77] Therefore, Equation 3.3 for the calculation of differential Raman scattering cross-sections can account for the angular dependence and can be directly compared to cross-sections measured using spontaneous Raman scattering.

The 2PA and differential Raman scattering cross-sections share the same dependence of the overlap factor (GF) based on the experimental overlap of the pump and probe pulses. By combining Equations 3.1 and 3.3, the absolute 2PA cross-section can be calculated without the overlap factor

(GF) of the pump and probe.

$$\sigma_{2PA}(E_{total}) = \frac{8\pi^3 c^2 N_{solvent}}{\omega_{probe}^2 N_{solute}} \left(\frac{d\sigma_{Raman}}{d\Omega}\right) \frac{\int \Delta A_{2PA}(\tau) d\tau}{\int \Delta A_{Raman}(\tau, \omega_{probe}) d\tau d\omega_{probe}} \tag{3.4}$$

The measurement of the stimulated Raman scattering can, therefore, act as an internal standard for the experimental uncertainty introduced from the overlap between the pump and probe pulse. If the differential Raman scattering cross-section is known for the specific vibration, the absolute 2PA cross-section can then be evaluated without the large uncertainty in the overlap. Therefore, a significant source of uncertainty in the measurement of the absolute 2PA cross-section can be removed.

3.3 Experimental Details

The broadband 2PA spectrum is obtained using the pump-probe method as described in earlier publications, which uses a pump and probe pulse overlapped both spatially and temporally within the sample.[58,76,78] The samples consisted of 13 mM solutions of coumarin 153 (Sigma 99%) dissolved in methanol, DMSO, and toluene. Both the pump and probe are derived from the fundamental 800 nm output of a commercially available 1 kHz regeneratively amplified Ti:Sapphire laser (Coherent, Legend Elite) using optical parametric amplification. The pump pulses were centered around 1150 nm and a pulse duration of 100 fs. The broadband probe pulses were generated by focusing 1200 nm light from a second OPA into a circularly translating 1 mm CaF_2 substrate to initiate continuum generation. The femtosecond white-light continuum (WLC) covered a range of 2.48 eV (500 nm) to 1.24eV (1000 nm) and was collimated and then focused using a pair of aluminum parabolic mirrors to a diameter of approximately 100 μm at the sample. The probe light is then dispersed using a transmission grating onto a 256-element photodiode array for broadband detection.

The pump beam is chopped at a frequency of 500 Hz blocking every other pulse for active background subtraction. A convex focusing lens in the pump beam is mounted on a translational

stage to adjust the overlap of the pump and probe focuses within the 1 cm sample cuvette. The pump beam is then crossed at a small angle less than 10 degrees between the WLC in the horizontal plane of the laser table. Attenuation of the pump pulse energy is achieved using a variable neutral density filter wheel between a range of 1 to 4 μJ per pulse to eliminate any transient absorption signal due to degenerate non-linear excitation from the pump beam.

A small delay range between the pump and probe is scanned to ensure that the temporally chirped probe pulse is overlapped with the pump pulse. The time-dependent absorption signal is measured by scanning the delay (τ) between the pump and probe pulses to measure both the 2PA and SRS signals simultaneously. Three scans of the time delay between the pump and probe and averaging over 2000 laser shots per time point to average the 2PA and SRS signals were used.

Separate stimulated Raman scattering measurements using a picosecond narrow bandwidth pump pulse were performed to better resolve the Raman scattering signals for comparison. The narrow bandwidth picosecond pump pulses were generated using spectral compression by second harmonic generation (SC-SHG) in a long β-barium borate (BBO) crystal and a 4f spectral filter to produce narrow bandwidth picosecond pump pulses as demonstrated by Pontecorvo et al. for SRS measurements.[67]

3.4 Results

The two-photon absorption spectra of coumarin 153 were measured using the broadband 2PA technique in multiple solvents with different polarity. The broadband 2PA method tracks both the pump-probe delay and the frequency dependence of the 2PA signal and is displayed as a 2-D plot of the ΔmOD signal as shown in Figure 3.3 for coumarin 153 in methanol. The ΔmOD signal is the same as pump-probe experiments where the change in absorption is the difference when the pump and probe are incident upon the sample, and when only the probe is incident. The broadband 2PA method, therefore, measures the attenuation of the white light probe continuum directly as a function of pump-probe delay(τ). The overlap of the pump and probe has multiple contributing signals from stimulated Raman scattering (SRS), cross-phase modulation (XPM), and the intended

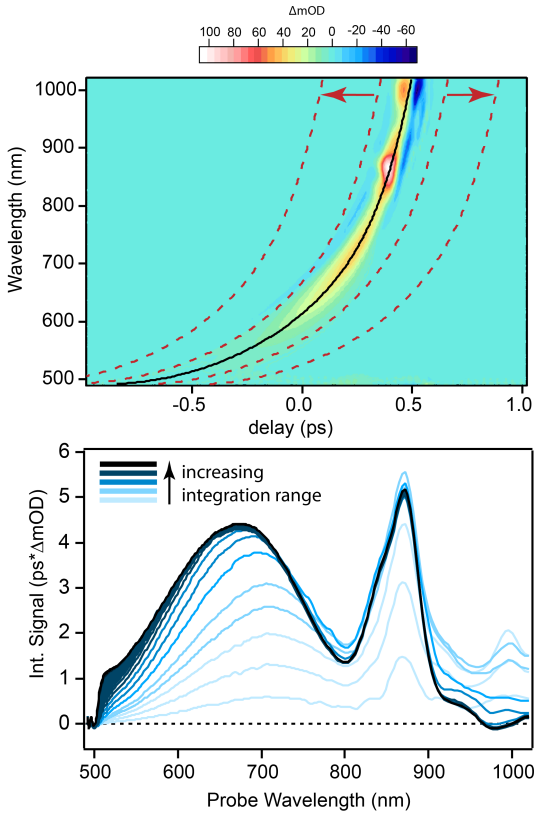

Figure 3.3: The contour plot representing the ΔmOD signal,as a function of probe wavelength and pump-probe delay (τ). The dashed lines represent the limits of integration over the pump-probe delay (τ) to obtain the time-independent 2PA spectrum. The two-photon absorption spectrum is shown as a function of the integration range.

two-photon absorption which are all observed in Figure 3.3. The two-photon absorption only occurs when the pump and probe are overlapped in time, and the combined energy of a pump and probe photon corresponds to an allowed 2PA transition in the sample. The observed signal in 3.3 takes a curved shape due to the group velocity dispersion(GVD) of the white light continuum. The wavelength-dependent index of refraction leads to the various wavelengths arriving at the sample at different times. Time zero (τ=0) at each wavelength is defined as the maximum overlap between the pump and probe pulses and is indicated in Figure 3.3 as the black trace. To recover the time-independent 2PA and SRS spectra, we integrate over the pump-probe delay (τ). The integration over the delay(τ) eliminates the contribution from dispersive features, like XPM of the WLC probe, and retains any absorptive or emissive features.[79,80] The integration ranges are varied to ensure complete integration of the 2PA signal as shown by the dashed red traces. The lower panel

of Figure 3.3 shows the dependence of the 2PA and SRS spectrum on the integration range.

The pump wavelength and range of the white light continuum were explicitly chosen to satisfy both the requirement for the total energy of the 2PA and the known Raman shifts of solvent to measure both simultaneously. The total energy of the combined pump and probe photons must be equal to an allowed 2PA transition in c153. In addition, the white light continuum must be close enough in frequency to the pump for the known Raman shift frequencies of the solvents to appear in the broadband 2PA measurement. Therefore, the SRS peaks shown in Figure 3.4 appear within the probe range at approximately 870 nm due to the known Raman shift frequencies for the C-H stretching of methanol. The observed stimulated Raman scattered photons are higher in energy compared to pump and therefore are anti-Stokes Raman scattering bands. The anti-Stokes Raman signals are an absorptive feature, which are positive in the calculation of the ΔA signals as shown in Figure 3.3. In the measurements of the coumarin (c153) solutions, both contributions from the 2PA of the solute and SRS of the solvents were observed. The 2PA shown in Figure 3.4 only has appreciable signal in the measurement of the c153 solutions and negligible signal for the measurements of pure solvents in the probe range from 500-800 nm. Two-photon absorption only occurs in the range where the total energy between the pump and probe corresponds to an allowed transition in a molecule.

The contributions from SRS, which are present in both measurements of the pure solvent and c153 solutions are shown in the blue traces of Figure 3.4. The resolution of SRS scattering signals in the broadband 2PA technique is limited by the use of a 100 fs pump pulse with approximately 150 cm^{-1} bandwidth; limiting our ability to resolve the individual Raman scattering bands. A separate SRS measurement of methanol was performed with a spectrally filtered picosecond pulse with 10 cm^{-1} bandwidth to resolve the individual Raman scattering peaks. The agreement between the SRS measurements using different bandwidth pump pulses shows that the signals from the broadband 2PA measurements are the C-H and O-H stretching Raman bands of methanol.

A series of measurements with varying solvents were taken using the broadband 2PA method and the same experimental conditions described previously. The 2PA spectra of coumarin 153 in

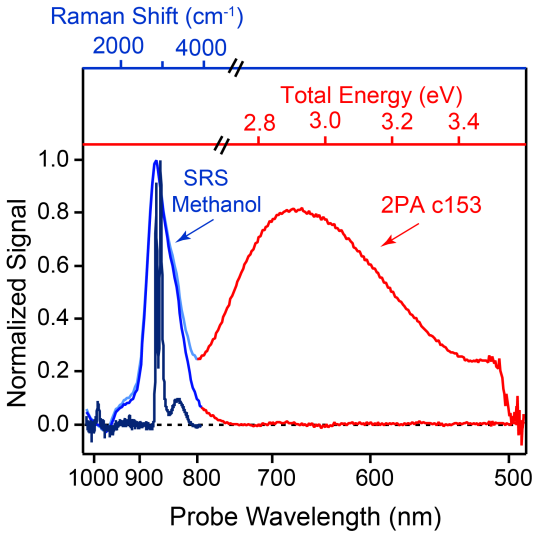

Figure 3.4: The normalized 2PA spectrum for c153 in methanol and the solvent only 2PA spectrum of methanol are plotted versus probe wavelength. The blue region corresponds to signals of SRS, which comes predominately from the solvent, and the red region corresponds to the 2PA of c153.The dark blue trace is a separate SRS measurement of methanol using narrow-bandwidth picosecond pump pulses to resolve the individual Raman scattering peaks.

methanol, DMSO, and toluene were collected in back to back to ensure minimal variation in the experimental conditions between each sample. The two-photon absorption spectra for each solution, the solvent only, and the solvent-subtracted spectra are shown in Figure 3.5. The solvent-only measurements for methanol, DMSO, and toluene are represented by the blue traces and only contain stimulated Raman scattering signals. The 2PA spectrum of each sample solution has contributions from both 2PA and SRS of the high-frequency C-H stretching modes of the solvent, as shown in the appendix (Figure 3.8). The contribution from the solvent and the SRS can be subtracted to obtain the 2PA spectrum of the different c153 solutions.

The 1PA and the solvent subtracted 2PA spectra of c153 in the different solvents are shown in Figure 3.6. The molecular symmetry determines both the one and two-photon allowed electronic transitions. Since coumarin 153 is a low symmetry molecule with C_1 point group, the 1PA and 2PA spectra of c153 in all solvents are similar showing that either a 1PA or 2PA process will reach the same electronic state. The broadband 2PA technique can reproduce the solvent shifting of the absorption bands seen in the 1PA spectra for each solution due to the different solvent interactions.

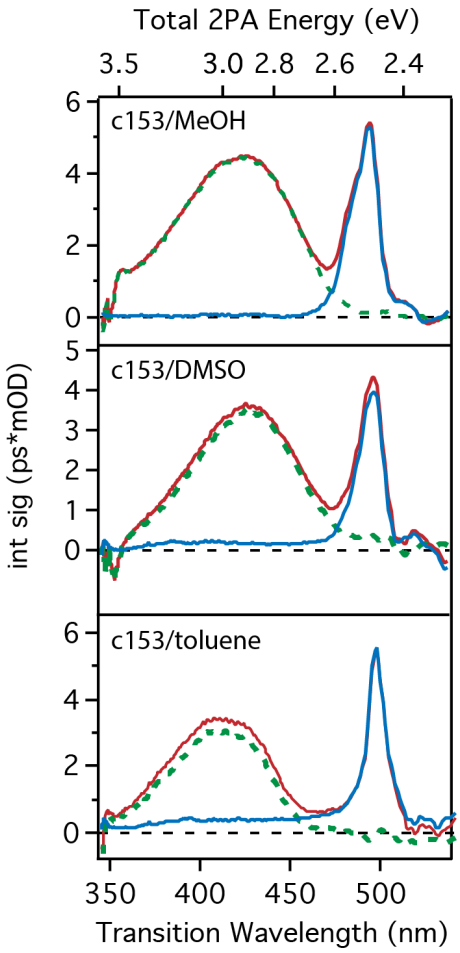

Figure 3.5: The two-photon absorption spectra of coumarin 153 in methanol, DMSO, and toluene are plotted as a function of (ps*mOD). The solvent only SRS spectra and the solvent subtracted 2PA spectra for each solution are shown.

Also, the different solvent interactions between the polar and non-polar solvents are apparent in the absorption band of the c153 solutions and are identical in both the 1PA and 2PA spectra. The ability for the broadband 2PA technique to not only accurately measure the subtle shifting due to solvation, but also the different spectral shapes based upon the different solvent polarity demonstrates why the broadband 2PA technique is a powerful spectroscopic tool.

The absolute 2PA cross-sections in Figure 3.7 are calculated using Equation 3.1. The overlap was estimated by measuring the individual beam diameters at the focus and calculating the overlap factor (*GF*), as shown in Equation 3.2. The absolute 2PA cross-sections based on the estimated overlap between the pump and probe are shown in Figure 3.7 as the blue traces for the series of

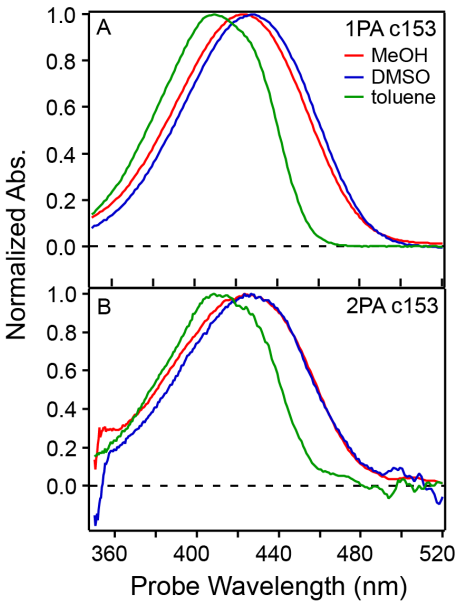

Figure 3.6: The one and two-photon absorption spectra for c153 in methanol, DMSO, and toluene.

solvents. To remove the dependence of the 2PA cross-section on the overlap between the pump and probe, the differential Raman scattering cross-sections were evaluated from the solvent SRS measurements. The absolute 2PA cross-section is corrected to compensate for the uncertainty in the spatial overlap by comparing the measured differential Raman scattering cross-section to a reference value from the literature. Table 1 contains the measured values for the differential Raman scattering cross-sections from our broadband 2PA measurements, as well as the value used as a reference standard. The differential Raman scattering cross-sections were calculated from our SRS measurements for three different solvents methanol, DMSO and toluene. A frequency-independent differential cross-section can then be calculated to compare Raman cross-sections measured at different Raman excitation wavelengths. The differential cross-section scales as $\approx \frac{1}{\omega_{pu}\omega_s^3}$ and can, therefore, be calculated independent of the Raman pump wavelength to allow for direct comparison between our results at 1158 nm and the value published in the literature for 488 nm Raman excitation.

We use the ratio between the differential Raman cross-sections measured using the broadband 2PA technique and a published value in the literature as shown in the work by Houk et al.[27] The ratio is called the correction factor as it is used to scale the absolute 2PA cross-sections to correct

Table 3.1: Raman cross-sections from broadband two-photon absorption measurements of coumarin 153

	Raman Pump	Diff. Raman Cross-section $\frac{d\sigma_{Raman}}{d\Omega}$ (a)	Freq. Ind. Raman Cross-section $\frac{d\sigma_{Raman}}{d\Omega} * \frac{1}{\omega_{pu}\omega_s^3}$ (b)	Correction Factor
Methanol [(c)]	488 nm	5.7 / 6.9[(d)]	52.0 / 63.0[(d)]	-
Methanol	1158 nm	0.34	45	1.4
DMSO	1158 nm	0.31	43	- [(e)]
Toluene	1158 nm	0.66	89	- [(de)]

[a] $*10^{-30}$ $(\frac{cm^2}{sr*molecule})$
[b] $*10^{-48}$ $(\frac{cm^6}{sr*molecule})$
[c] Griffiths *et al.*[81]
[d] Differential Raman cross-section adjusted for contribution of O-H band
[e] From Methanol measurement assumes same overlap conditions between measurements

for systematic error in estimating the overlap of the pump and probe. In the methanol measurement, a reported literature value is used as the reference for the correction ratio.[81] In the absence of a reported literature value for a specific Raman scattering cross-section, the measurements of the different solvents were taken back to back to ensure minimal differences in the experimental conditions. Therefore, the correction factor calculated from the measured differential Raman scattering cross-sections for methanol can be directly applied to the DMSO and toluene measurements. In the case of methanol, we calculated the differential Raman cross-section for our comparison by taking the sum of the reported cross-sections for the three Raman bands observed in Figure 3.4 because we could not resolve the individual bands in the measurements using a femtosecond pump pulse.[81] The observed Raman bands correspond to the C-H and O-H stretching modes of the methanol. The differential Raman cross-section for methanol was adjusted to account for the O-H stretching band by taking the ratio of the area under each Raman band, as shown in the appendix (Figure 3.9). The correction factor can be calculated by taking the ratio of the frequency-independent Raman cross-sections from our results and the value from the literature, and then directly applied by multiplying 1.4 to solvent subtracted 2PA c153 solution spectra, resulting in the green traces in Figure 3.7.

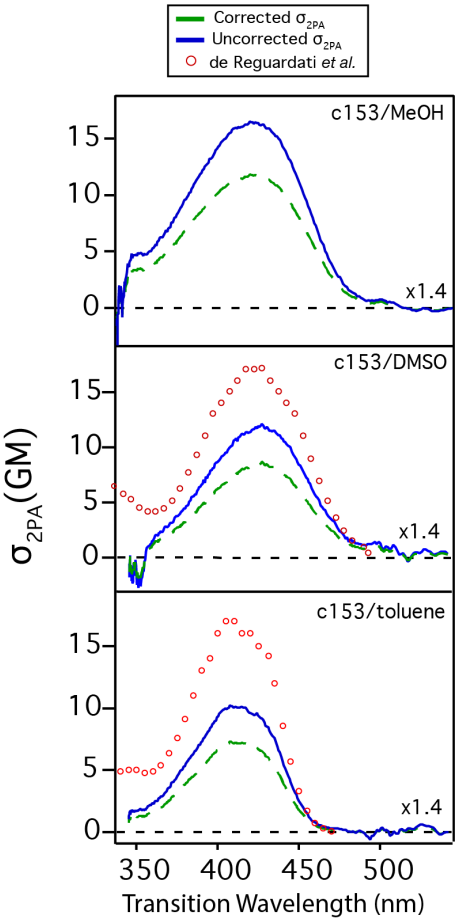

Figure 3.7: The two-photon absorption spectra of c153 in methanol, DMSO, and toluene measured using the broadband 2PA technique. The absolute 2PA cross-sections for c153 are shown with the correction from the internal standard of SRS and without.The two-photon absorption cross-sections measured by De Reguardati et al.[54] are shown for comparison.

Previously reported values for the absolute 2PA cross-sections for c153 in DMSO and toluene by DeReguardatti *et al.*[54] using a two-photon fluorescence measurement agree with the absolute 2PA cross-sections measured using the broadband 2PA technique. Also, the spectral shape of the 2PA band for both solvents are reproduced using the broadband 2PA style measurement.

3.5 Discussion

The broadband 2PA technique measures continuous 2PA spectra and accurate absolute 2PA cross-sections. The pump-probe derived nature of the technique makes it easily implemented on any ultrafast laser system. Often, the intensity profiles of ultrafast laser pulses complicate the measurement of the absolute 2PA cross-sections leading to large uncertainties. The broadband 2PA method, as demonstrated, takes advantage of the internal standard of SRS of the solvent to correct for systematic errors in the measurement of the absolute 2PA cross-section without the need for additional reference standards.

The implementation of the broadband white light continuum measures the broad spectral dependence of the 2PA signal in a single measurement without tuning the wavelength of the laser. It also eliminates changes to the experimental setup and reduces the introduction of systematic errors such as the change in the intensity profile of the laser pulses as they are tuned. The ability to capture the entire 2PA spectrum in a single measurement reduces the experimental time needed. Additionally, the white light continuum allows for the simultaneous measurement of the differential Raman scattering cross-sections for use as an internal standard.

The absolute 2PA cross-sections and differential Raman scattering cross-sections measured in this work agree well with the reported values in the literature even when considering the assumptions made in estimating the overlap between the two laser pulses. The overlap factor (GF) in equation 1 assumes that two collimated collinear laser pulses are overlapping over a small path length. In the measurements presented in this work, the pump and probe pulses crossed at a small angle and overlapped within a 1 cm cuvette. The large path length helped to reduce the effect from XPM from the windows of the cuvette, and the integration over the temporal domain takes into account the GVD introduced by the large path length.

3.6 Conclusions

Utilization of the stimulated Raman scattering as an internal standard within broadband two-photon absorption technique can improve upon an already powerful spectroscopic technique by increasing the accuracy of the absolute two-photon absorption cross-sections. The broadband two-photon absorption technique demonstrated above was able to resolve the shift due to polar and non-polar solvents, as well as the small changes in the absorption band derived from the solvent interactions as seen in the measurements of coumarin 153 in toluene. The need for materials that undergo non-linear transitions readily are limited by the current two-photon absorption spectroscopic techniques; however, this pump-probe derived method combines the accurate cross-section measurements usually restricted to single wavelength two-photon absorption cross-section measurements with a high-density of wavelength measurement allowing for more accurate non-linear spectroscopy. With improved methods of non-linear spectroscopy, the study and eventual synthesis of materials for the applications in microscopy and photo-therapy will continue to advance.

3.7 Appendix

The stimulated Raman spectra of each of the solvents were measured using both a femtosecond and picosend pump pulse. The bandwidth limited femtosecond measurement is shown as the blue traces, and the red traces correspond to the spectrally filtered picosecond pump pulse measurements shown in Figure 3.8. The spectrally filtered picosecond pump measurement clearly demonstrates that the poorly resolved femtosecond measurements convolute the high-frequency Raman bands of each solvent.

The differential Raman cross-section for methanol was measured using a femtosecond pump pulse, and the individual Raman bands were not resolved due to the large bandwidth of the femtosecond pump pulse. Therefore, to compare the experimentally measured differential Raman cross-section for methanol, which includes the contribution from all three observed Raman bands, the sum of the reported cross-sections was taken. The differential Raman cross-section for the two

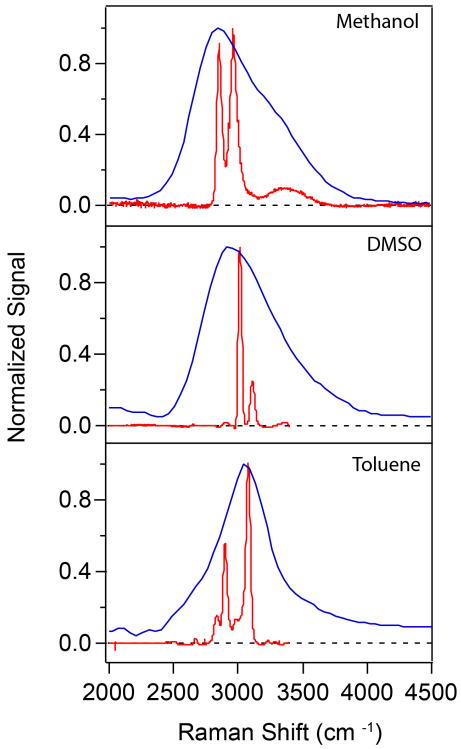

Figure 3.8: The high-frequency Raman bands from methanol, DMSO,and toluene measured with both femtosecond and picosecond pump pulse

C-H stretching vibrations was published by Griffiths *et al.*; however, the cross-section for the weak O-H stretch was not measured.[81] Therefore to accurately reflect our measurement of the differential Raman cross-section the integrated area beneath the individual Raman bands were compared, as shown in Figure 3.8. By taking the ratio of the integrated areas the differential Raman cross-sections reported by Griffiths *et al.*[81]can be corrected to include the contribution of O-H band. This was to ensure a good comparison between femtosecond measurements and the literature. The values of the summed differential cross-sections and the correction for the O-H band are shown in Table 3.1.

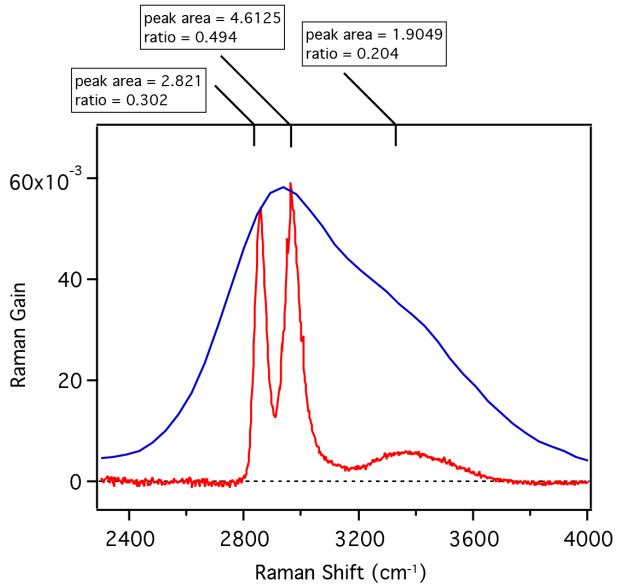

Figure 3.9: Integrated areas of the high-frequency Raman bands of methanol to correct for contributions from the O-H band to the differential Raman cross-section.

Chapter 4

Broadband Two-Photon Absorption Spectroscopy of Liquid Benzene: Resolving Vibronic Structure in the Electronically Forbidden $B_{2u} \leftarrow A_{1g}$ Transition

4.1 Introduction

Two-photon absorption is often acknowledged for the different electronic selection rules which can allow access to one-photon forbidden electronic states. The allowed electronic transitions in molecules are described by the molecular symmetry and the point group of the molecule. In the specific case of centrosymmetric molecules, two-photon absorption can lead to excited electronic states that are one-photon forbidden by the parity selection rule. Two-photon absorption in centrosymmetric molecules allows transitions from either gerade to gerade state or an ungerade to ungerade state that is formally forbidden for one-photon absorption.[31,82] Therefore, 2PA processes in centrosymmetric molecules allow access to additional electronic states unavailable to 1PA absorption, making 2PA an attractive method for initiating chemical reactions. The products of photochemical reactions are known to be affected by the wavelength of excitation and the excited state dynamics, therefore the access to different electronic state through two-photon allowed transitions can be used to control photochemical reactions.[83] For this reason, studies have been carried out on a variety of molecules looking to use two-photon absorption to control the photochemical reactions.[27,36,43] In addition, many other applications also use the properties of two-photon absorption as mentioned previously in chapter 1. Therefore, novel 2PA chromophores and detailed understanding of the two-photon absorption spectroscopy are needed.

The stimulated Raman scattering was shown to be a valuable internal standard that can be measured simultaneously with the two-photon absorption signal to correct for experimental uncertainty. However, the measurements made with femtosecond pump pulses poorly resolve the stimulated Raman scattering signals due to the bandwidth of the femtosecond pump pulse. The stimulated Raman scattering signal inherently has bandwidth based upon the dephasing lifetime of the vibrational coherence, and when the bandwidth of the pump pulse exceeds the natural line width, broadening of the vibrational signal occurs.[84] Specific techniques that have been developed, such as femtosecond stimulated Raman Scattering, have been used to study the ultrafast vibrational evolution of molecular systems.[65,77] There has been work in the development of narrow-bandwidth picosecond pulses to be used in stimulated Raman scattering measurements to eliminate artificial signals and broadening.[67,85–87]

In order to test the resolution of the broadband two-photon absorption technique, benzene was chosen as a proof of principle system due to its well known one-photon absorption and two-photon absorption spectroscopy. The one-photon absorption and two-photon absorption spectroscopy of benzene have been well studied by many researchers in the past 70 years. Benzene belongs to the point group D_{6h} and is a highly symmetric molecule making it a spectroscopically interesting for both one-photon and two-photon absorption spectroscopy. The one-photon absorption spectrum of benzene was measured in the near-ultraviolet region from 200-280 nm by Sponer *et al.*[88,89] The weak absorption in this region and the vibronic structure are due to a forbidden electronic transition $B_{2u} \leftarrow A_{1g}$ that requires coupling of vibrational motion of a specific symmetry in order for the absorption to become weakly allowed. Sponer *et al.* assigned the multiple vibronic progressions in the one-photon absorption spectrum for this region. The spacing in the vibronic progressions is determined by the vibrations that are coupled to weakly allow the forbidden electronic transition, and therefore different symmetry vibrations are responsible for the absorption in the two-photon absorption spectrum of benzene. This made benzene spectroscopically interesting target molecule for both 1PA and 2PA studies.

The two-photon absorption spectroscopy of the $B_{2u} \leftarrow A_{1g}$ of benzene was studied by many

researchers in both the gas and crystal phase looking to measure the different symmetry vibrations that lead to the vibronic progressions in the two-photon absorption spectrum. The two-photon absorption spectroscopy was measured with high resolution by Hochstrasser *et al.* and Wunsch *et al.* in the mid-1970s, where they were able to assign the transitions in the 2PA spectrum of benzene.[90–95] The condensed phase two-photon absorption spectrum of benzene of the $B_{2u} \leftarrow A_{1g}$ transition was also reported by Rice *et al.*[96] The well known vibronic structure, and progressions make it an ideal molecule to test the ability of the broadband 2PA technique to resolve the narrow vibronic peaks in benzene, but also to resolve the different symmetry vibrations that contribute to the observed vibronic progressions in the two-photon absorption spectrum of benzene.

In this chapter, the broadband two-photon absorption technique is used to study the benzene 2PA spectrum in the near-ultraviolet region. The 2PA of benzene is presented here both using a femtosecond and picosecond pump pulse. The use of narrow-bandwidth picosecond pump pulses eliminates the broadening of the stimulated Raman Scattering signals and shows the natural linewidth of the two-photon absorption signal in the condensed phase of benzene. In addition, the polarization dependence of both the two-photon absorption and stimulated Raman scattering are shown.

4.2 Experimental Details

The two-photon absorption spectrum of liquid benzene (Sigma 99%) was measured using the pump-probe derived broadband 2PA technique. As described in chapter 2, the technique uses two different ultrafast laser pulses overlapped in time and space within the sample. The measurements presented here were taken using a one-centimeter quartz cuvette. The first pulse, denoted as the pump pulse, is tuned to a single wavelength and required to be non-resonant with any electronic transitions in the sample. The probe pulse is a broadband white light continuum generated by focusing infrared 1200 nm output from an optical parametric amplifier (OPA) or fundamental 800 nm from a commercial laser system into a rotating CaF_2 substrate to generate continuum with

a range 350 - 1000 nm. The region of the two-photon absorption spectrum that is measured is fixed by the combined total energy of the pump and probe photons.

The pump and probe pulses are tightly collimated and crossed at a small angle, usually less than ten degrees within the sample, in order to ensure the maximum interaction between the two pulses. The generation of the broadband continuum introduces group velocity dispersion (GVD) across the white light continuum. The separation of the probe photons in time requires the use of optical delay stages and scanning of the pump-probe delay in order to capture all of the two-photon absorption and stimulated Raman scattering signals. The scanning of the time delay and time-dependent dispersive signals like cross-phase modulation (XPM) complicate the broadband 2PA technique. The XPM signals overlap with the 2PA and SRS signals and make difficult to directly observe the two-photon absorption signal. The contribution from dispersive XPM is eliminated from the final two-photon absorption spectrum by the integrating over the pump-probe delay.[79]

The picosecond pump pulse is generated using second harmonic spectral compression of the fundamental 800 nm pulses. The fundamental pulse is passed through a 1 cm β-barium borate (BBO) crystal that produces a stretched pulse in time at twice the incident frequency.[67] The spectrally compressed pulse has an asymmetric intensity profile in the temporal domain due to the second harmonic pulse propagating slower compared to the incident beam through the BBO. Therefore the asymmetric temporal pulse shape gradually increases over time and is followed by a steep drop off that lead to artificial signals in the stimulated Raman scattering signals. In order to eliminate the asymmetric temporal profile, a 4f spectral filter was used to remove the asymmetric intensity profile and reduce the overall bandwidth of the picosecond pump pulse.[67]

Two detection schemes were used in measuring the two-photon absorption spectrum and stimulated Raman scattering of neat benzene. The measurements using the femtosecond pump pulses were recorded by dispersing the white light continuum onto a 256-pixel silicon photodiode array (PDA). The continuum is dispersed using a 300 (lines/mm) transmission grating. The picosecond pump pulse measurements used a 1/8 m spectrograph with a 2068 pixel linear charge-coupled device (CCD) from Hamamastu. The white light is passed through a 150 μm slit and onto a 600

(lines/mm) reflection grating and dispersed onto the CCD detector. The combination of the narrow-bandwidth picosecond pump and the spectrograph allows for better resolution of the 2PA and SRS signals. The increased resolution is due to a combination of reducing the bandwidth of the pump pulse and increasing the dispersion of the probe photons using the spectrograph.

4.3 Results and Discussion

The broadband two-photon absorption spectrum of liquid benzene was measured using both a 400 nm pump pulse and a broadband white light continuum (450-750 nm) probe. The 2-D contour plots in Figure 4.1 shows the transient absorption signal (ΔmOD) signal as a function of the probe wavelength and the delay (τ) between the pump and probe pulses. The dashed trace in Figure 4.1, shows "time zero" (t_0) where the pump and the probe are at the maximum of their overlap in time. The 2PA spectrum of benzene is obtained by integrating over the pump-probe delay around t_0. Integrating only over the region around time-zero, allows for minimal inclusion of the signal fluctuations before and after t_0. The measurement of the two-photon absorption spectrum of benzene was measured using the broadband 2PA technique first with a fs 400 nm pump pulse and secondly with a ps 400 nm pump pulse. In Figure 4.1 the 2-D contour plots are shown for both the fs and ps pump pulses. A 1-D cut at 690 nm shows the temporal domain for comparison between the ps and fs 400 nm pump pulses in Figure 4.1. The largest difference between the two contour plots in Figure 4.1 is the linewidth of the stimulated Raman scattering peaks at 450 nm. In the picosecond pump case the narrow Raman band is well resolved. The femtosecond pump pulse measurement sill has the same contributions from the stimulated Raman scattering however the resolution of the Raman band is limited by the bandwidth of the fs pump pulse.

The time-integrated 2PA and SRS signals are shown in Figure 4.2. The vibronic structure is evident in the 2PA spectrum for the forbidden transition $B_{2u} \leftarrow A_{1g}$ in benzene. The electronically forbidden transition is only allowed through vibronic coupling. The forbidden transition of benzene has been studied in both the one-photon and two-photon absorption spectra. The spe-

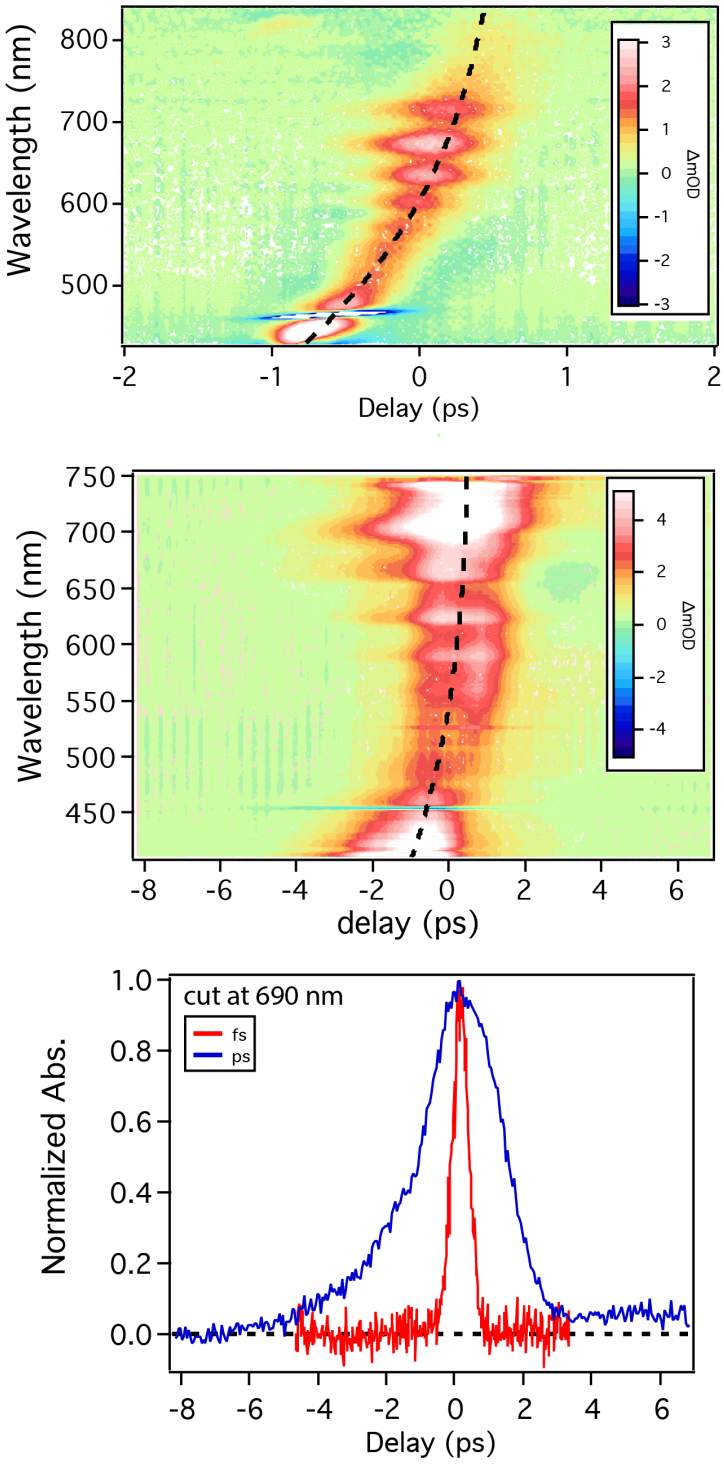

Figure 4.1: Contour plots produced from a broadband 2PA measurement of benzene measured with both a femtosecond and a narrow-bandwidth picosecond pump pulses with corresponding time cuts at 690nm

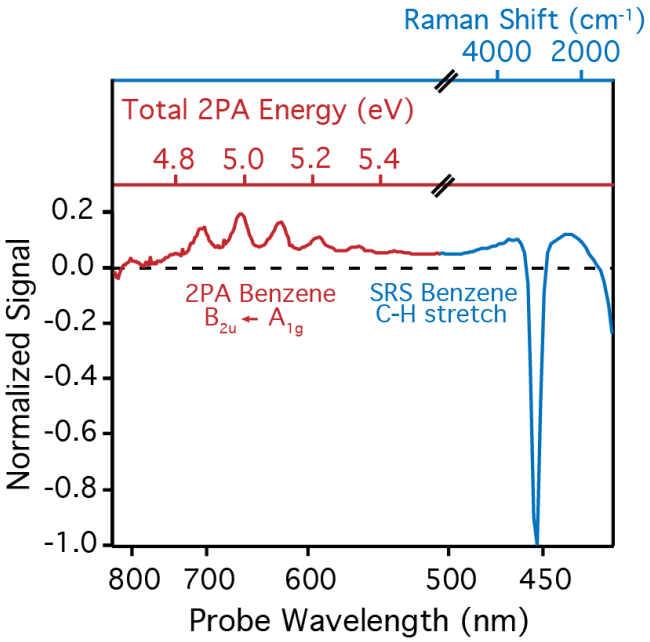

Figure 4.2: Broadband 2PA spectrum of the $B_{2u} \leftarrow A_{1g}$ transition in neat benzene using a fs 400nm pump pulse

cific molecular vibrations that lead to the vibronic progressions in each spectrum were assigned previously.[88–91,96] The other signal corresponds to anti-Stokes SRS signals of the C-H stretching modes of benzene and appears in Figure 4.2 as the large negative signal. In addition there is also overlapping SRS and a broad 2PA signal in the region above 5.4 ev as shown in figure 4.2.

The SRS scattering can be used as an internal standard, as demonstrated in Chapter 3, to correct for uncertainties in overlap between the pump and probe for the calculation of the absolute 2PA cross-section. The differential Raman scattering cross-section for the 3061 cm^{-1} band of benzene is proportional to the integrated area of the Raman band in the frequency domain. We calculate the differential Raman scattering cross-section from the TA signal using equation 3.3. A frequency-independent differential Raman scattering cross-section can be obtained using the approximate frequency dependence $(\frac{1}{\omega_{pu}\omega_s^3})$. The frequency-independent differential Raman scattering cross-section can then be directly compared to a known value from the literature measured at a different Raman excitation wavelength.[97,98] The ratio between the measured frequency-independent differential Raman scattering cross-section and the literature value can be used as a correction factor to

compensate for the error in the estimation of the pump-probe overlap, as demonstrated in chapter 3. The measured and reference values for Raman cross-sections used as an internal standard are found in table 4.1.

The resolution of the SRS signal in Figure 4.2 is limited by the large bandwidth of the 75 fs

Table 4.1: Raman cross-sections for the 3061 cm^{-1} band of benzene measured using broadband two-photon absorption technique

	Raman Pump	Diff. Raman Cross-section $\frac{d\sigma_{Raman}}{d\Omega}$ (a)	Freq. Ind. Raman Cross-section $\frac{d\sigma_{Raman}}{d\Omega} * \frac{1}{\omega_{pu}\omega_s^3}$ (b)	Correction Factor
Benzene[(c)]	441.6 nm	68.8	404	-
Benzene (fs)	398 nm	15.1	56	7.2
Benzene (ps)	398 nm	21	77	5.2

[a] $*10^{-30}(\frac{cm^2}{sr*molecule})$
[b] $*10^{-48}(\frac{cm^6}{sr*molecule})$
[c] Schomacker *et al.*[98]

pump pulse. The incorporation of narrow bandwidth picosecond pump pulses reduces the Raman excitation bandwidth, and therefore can better resolve the stimulated Raman scattering signals.[67,85] The 2PA spectra of benzene measured using fs and ps 400 nm pump pulses are compared in Figure 4.3. The broadband 2PA spectrum of benzene as a function of the absolute 2PA cross-section for the electronically forbidden 2PA transition is about 1 GM. The upper panel of Figure 4.3 shows only the 2PA spectrum of benzene measured using the two different pump pulses, and the lower panel shows the normalized SRS signals for each pump pulse. The use of a narrow-bandwidth 1 ps pump pulse increased the resolution of the SRS signal in the broadband 2PA measurement when compared to the fs measurement, as shown in Figure 4.3. The 2PA signal in the upper panel of Figure 4.3 is unchanged when measured using the narrow bandwidth picosecond pulse. The unchanging linewidth is due to the resolution being limited by the natural linewidth of the solution phase measurement and not the bandwidth of the pump pulse.

The picosecond pump pulse also has additional benefits to the broadband 2PA technique, such

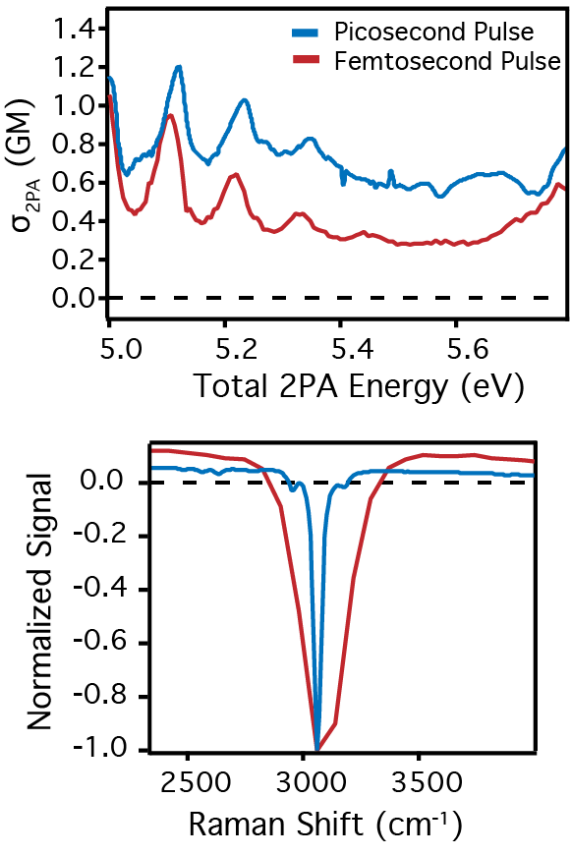

Figure 4.3: The broadband two-photon absorption spectrum of benzene using both a femtosecond and picosecond pump pulse.

as reducing the contribution from cross-phase modulation (XPM) by spreading the signal over a longer pulse duration. In addition, the longer pulse duration means that the entire chirped WLC simultaneously interacts with the picosecond pump pulse and reduces the amount of pump-probe delay that needs to be scanned or eliminate the need for scanning in the pump-probe delay entirely to measure the 2PA spectrum.

The broadband 2PA technique was able to measure and resolve the forbidden electronic transition in benzene. The electronic transition between the $B_{2u} \leftarrow A_{1g}$ state in benzene has been studied, and the nature of the transitions as well as the vibrations are well understood.[88,89,94–96,99] The assignments in both Figures 4.4 and 4.5 match the assignments from Sponer *et al.* for the 1PA spectrum and Rice *et al.* for the 2PA spectrum.[88,96] In Figure 4.4, the 1PA and 2PA spectra are shown as a function of transition frequency (cm^{-1}) to show the vibrational progressions as

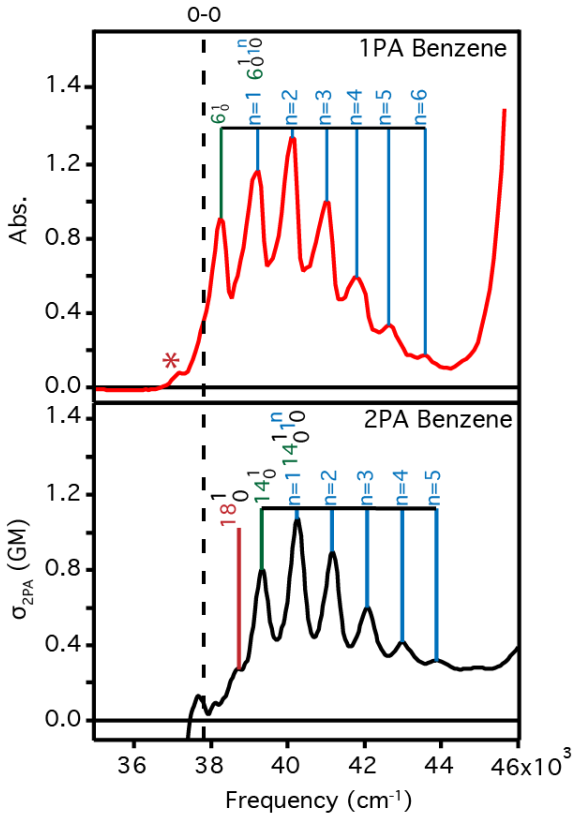

Figure 4.4: The one-photon and two-photon absorption spectrum of benzene as a function of transition frequency with the assignment of the vibronic progression

well as the location of the 0-0 band in benzene, which is a symmetry forbidden vibronic transition. The energy level diagram in Figure 4.5 shows the vibronic progressions for both the 1PA and 2PA spectra. The inducing vibration in the 1PA transition is the normal mode ν_6, which has E_{2g} symmetry. The progression to higher energy is attributed to the ν_1 normal mode with a symmetry assignment of A_{1g} for the 1PA spectrum. Similarly, in the 2PA transition, the inducing vibration is the ν_{14} normal mode having B_{2u} symmetry, with the progression being built upon the ν_1 normal mode in the same way as the 1PA spectrum. The broadband 2PA technique was able to resolve the vibronic structure in the benzene 2PA spectrum with enough resolution to assign the vibrational progressions and the 0-0 band.

Lastly, the broadband 2PA technique being a two-pulse technique allows for measurement of the polarization dependence of both the 2PA and SRS signals. The polarization dependence of Raman scattering is often reported as a depolarization ratio (ρ), which is defined as the ratio of the

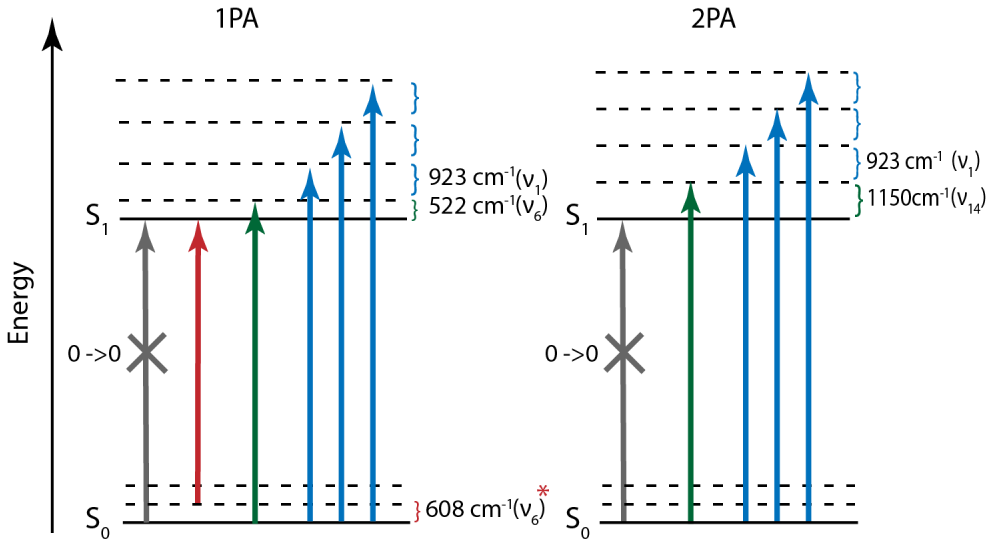

Figure 4.5: Energy level diagram of the vibronic progressions in the one and two-photon absorption spectra

perpendicular signal to the parallel, shown by equation 4.1.

$$\rho = (\frac{\Delta A_{\perp}}{\Delta A_{\parallel}}) \tag{4.1}$$

The depolarization ratio for a transition is dependent upon the molecular symmetry and therefore the point group to which it is assigned. The depolarization ratio can theoretically have any value between zero and infinity, but most commonly, it has a value of 0.33 or 0.75. The depolarization ratio for totally symmetric vibrations is generally between 0 and 0.75 and the non-totally symmetric vibrations are greater than 0.75.[84,100]

The stimulated Raman scattering signals measured using the broadband 2PA technique in figure 4.6 has an intermediate depolarization ratio of 0.5. The polarization dependence of the high-frequency C-H stretching modes has been studied previously and reported by Proffitt *et al.*[101] The C-H stretching Raman bands of benzene include two transitions at 3045 and 3062 cm^{-1}. Reported by Proffitt *et al.* the polarization dependence these bands at 3062 cm^{-1} band is depolarized with a ratio of $\rho = 0.11$ and 3045 cm^{-1} band has a depolarization ratio of $\rho = 0.53$. Since the measured stimulated Raman scattering signal in Figure 4.6 contains both C-H stretching Raman bands

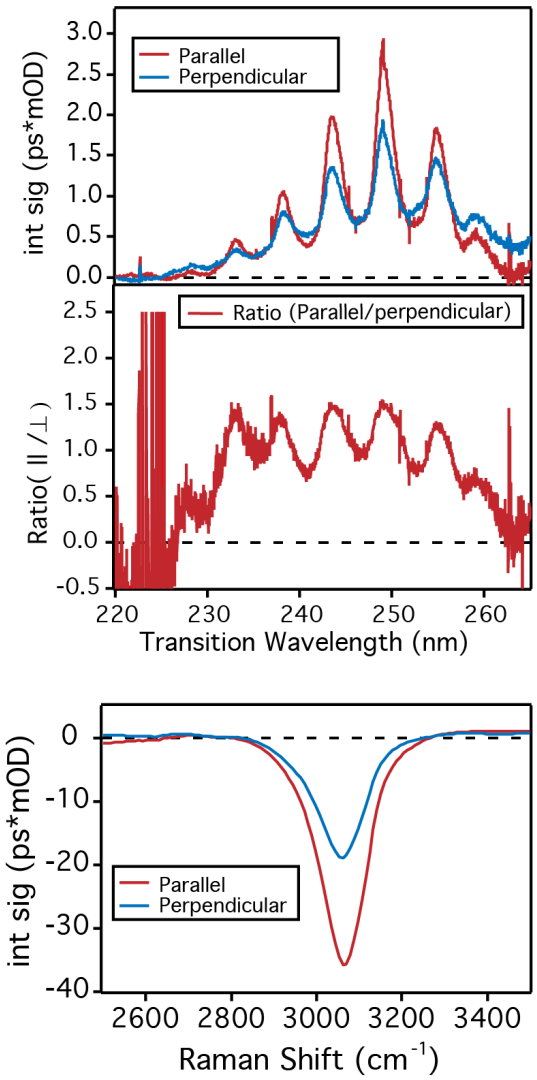

Figure 4.6: Polarization dependence of the two-photon absorption and stimulated Raman scattering of benzene

the weighted average can be used to estimate the expected depolarization ratio for the combined bands. The weighted average from the known depolarization ratios estimated the combined depolarization ratio to be 0.3. The measured depolarization ratio of 0.5 can be explained by the limited polarization purity achieved during this measurement. Even with the limited polarization purity the stimulated Raman scattering can still be used as an internal standard for the calculation of the absolute 2PA cross-section. In addition, the stimulated Raman scattering can also provide insight into the polarization dependence of the two-photon absorption measurement. The stimulated Raman scattering signals can also be used as an internal standard if the polarization dependence of the

measured solvent Raman bands is known. Therefore, the stimulated Raman signals can be useful in the calculation of the 2PA cross-sections as well as the polarization dependence measurement of the two-photon absorption signals.

4.4 Conclusions

The development of the broadband two-photon absorption technique through the implementation of picosecond pump pulses provides for a wide range of benefits for the development of this technique. The picosecond pump pulse improved the capability of the broadband two-photon absorption technique to resolve the narrow Raman signals by reducing the overall bandwidth of the pump pulse. The comparison of the picosecond and femtosecond pump pulses clearly shows the improved ability of the technique to resolve the Raman signals. The resolution of the Raman scattering signals is no longer limited by the bandwidth of the pump pulse but instead by the method of detection and the inherent line width of the Raman signal. In addition, the amplitude of the cross-phase modulation signal is stretched over a longer pulse duration and is hardly noticeable when using a picosecond pump pulse. Therefore, the identification of the signals derived from two-photon absorption becomes easier. Lastly, the largest complication of the broadband two-photon absorption technique is the use of optical delay stages to account for the chirped white-light continuum. The longer pulse duration enables the interaction of the pump pulse with a broader range of chirped probe wavelengths at a single pump-probe delay.

The two-photon absorption spectrum of the A_{1g} to B_{2u} transition in benzene was measured using the broadband two-photon absorption technique. The forbidden electronic transition in benzene was chosen for measurement because of its known vibronic structure in order to test the ability of the broadband two-photon absorption to resolve the vibronic structure in the condensed phase. The broadband two-photon absorption technique can not only resolve the vibronic progressions, but it could also resolve the different inducing vibrations.

Chapter 5

Future Directions

5.1 Development of Single Shot Two-Photon Absorption Measurement

The largest complication in the measurement of a two-photon absorption spectrum is the necessity of ultrafast laser pulses for all the techniques mentioned in this thesis. They are complicated by either the use of translational stages or by tuning of laser wavelengths. The broadband 2PA technique requires the use of optical delay stages in order to overlap the ultrafast laser pulses in time. The z-scan technique's use of translation stages is required to move the sample through laser focus. The work presented in this thesis has been to develop the broadband two-photon absorption technique in order to reduce the experimental uncertainty using stimulated Raman scattering as an internal standard, and to reduce the complexity of the technique by incorporating picosecond pump pulse.

Motivated by the idea of a single shot two-photon absorption measurement single-shot techniques have been demonstrated previously, and most notably the frequency-resolved optical gating(FROG) techniques that have been developed to simultaneously measure the time and frequency domains of ultrafast laser pulses. The FROG technique can be implemented in a variety of different schemes based on the beam geometries, and how the optical gating is occurring. For example, the FROG technique can be used in second-harmonic generation FROG (SH-FROG) geometry, four-wave mixing in the transient grating FROG (TG-FROG) and others.[64,102,103] The most important feature of the FROG autocorrelation measurements is the ability to encode both the time and frequency domains in a single-shot measurement. Similarly, a single shot two-photon absorption measurement could be possible if the combination of the stretched picosecond pump pulses

and simultaneous measurement of the time and frequency domains as demonstrated in the FROG measurements.

We previously implemented for diagnostic purposes the polarization-gated frequency-resolved optical gating (PG-FROG) as demonstrated by Trebino et al. The PG-FROG was implemented as diagrammed in the schematic in Figure 2.1.[63,104] The PG-FROG setup requires two beams where the polarization is rotated 45 degrees between the two. The beams are then overlapped in time and space inside of a fused silica substrate. The mapping of the temporal domain comes from the use of a cylindrical lens and line focus. By focusing to a line, the temporal information is encoded spatially as the two laser pulses propagate through the medium, as shown in Figure 5.1. The beam with the polarization that is rotated 45 degrees is discarded. The other laser beam is

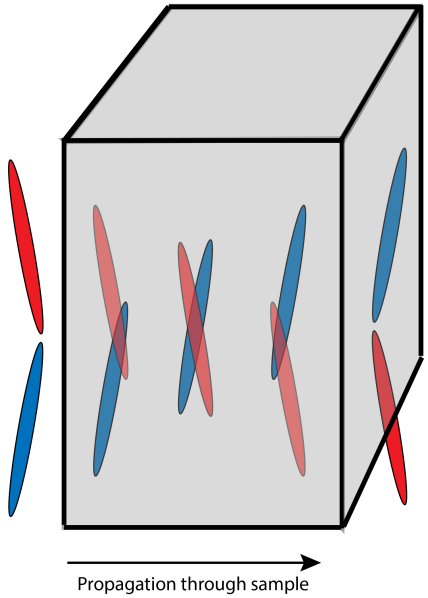

Figure 5.1: Representation of the time domain encoded spatially using overlapping pulses focused to a line.

put incident upon a perpendicular Glan-Taylor polarizer, therefore, cutting out the intensity before the reflection grating. Then as the two pulses interact in the fused silica substrate, the optical Kerr effect can rotate the polarization and allow for the FROG signal to pass through the polarizer and be dispersed onto the CCD detector.

The spectrogram of the transformed limited ultrafast laser pulse from the commercial regenera-

tively pumped Ti:Sapphire laser was measured using the PG-FROG autocorrelation measurement, and shown in the top spectrogram of Figure 5.3. The PG-FROG technique, as described, was able

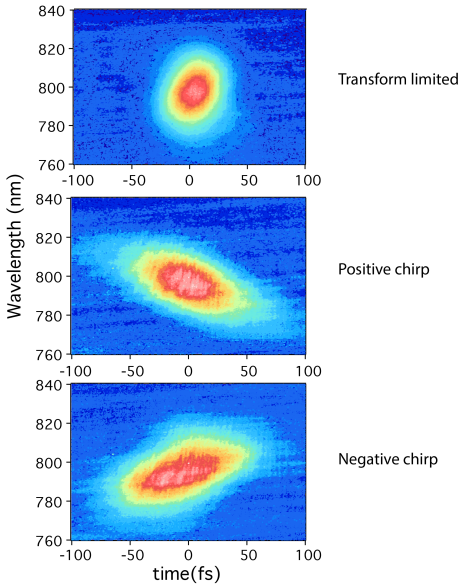

Figure 5.2: Spectrogram of an ultrafast laser pulse measured using PG-FROG

to measure the time and frequency domains of the ultrafast laser pulse. In addition, the single shot nature of the technique allowed for a live view of the group velocity dispersion or "chirp" of the laser pulse, as shown in the bottom spectrogram of Figure 5.3. The chirped laser pulses clearly show the dispersion of the pulse in time. The ability to visualize the spectrogram of the laser pulse without the complexity of optical delay stages is the reason why FROG instruments are a powerful diagnostic tool in the field of ultrafast laser spectroscopy.

The ability to measure broadband two-photon absorption spectra in a single shot would allow for the measurement of the 2PA spectrum without scanning the pump-probe delay or translation of the sample in the z-scan. Therefore would provide a simpler overall technique that can be used to move the entire field of study and the fundamental two-photon absorption spectroscopy. In addition, the single-shot measurement would significantly decrease the overall signal averaging by reducing the number of laser pulses needed to measure the complete two-photon absorption spectrum. The single-shot two-photon absorption spectrometer would increase the number of research groups that could actively measure accurate two-photon absorption, not just the limited number of

researchers with transient absorption capabilities.

5.2 Two-Photon Absorption Spectroscopy of Carbon Monoxide Releasing Molecules (CORMs)

The method development of the broadband two-photon absorption technique was ultimately to utilize this improved technique in measuring spectroscopically interesting molecules and working towards controlling photochemical reactions using two-photon absorption.[27] The use of two-photon absorption in photodynamic therapy (PDT) has been demonstrated and well studied due to the high spatial control granted from nonlinear absorption, and the better tissue penetration from wavelengths in near IR range.[14,15] The development of two-photon sensitizers for photodynamic therapy has be demonstrated in a wide variety of transition metal complexes including, metal carbonyl complexes. Metal carbonyl complexes have been shown to undergo carbon dioxide release after optical excitation of a metal to ligand charge transfer state.[105,106] Carbon monoxide has been shown to act as an intracellular signalling molecule and can be used to signal for many biologically beneficial behaviors such as anti-inflammation. The incorporation of non-linear absorption to the photochemical release of carbon monoxide is vital due to the well known general toxicity of carbon monoxide. The use of two-photon absorption can ensure that the carbon monoxide is produced in a tight focal volume and a non-harmful manner overall.

In order to better understand the carbon monoxide release in metal complexes, we did a preliminary study on a series metal carbonyl complexes with known carbon monoxide releasing behavior and the desired photoinduced carbon monoxide release is shown in figure 5.3.The preliminary series included both rhenium and manganese complexes. The rhenium complexes were used as a test molecule due to their photostable behavior and therefore, an overall more straightforward introduction to the two-photon absorption spectroscopy of metal complexes. Broadband two-photon absorption spectroscopy was used to better understand the photo-induced release of carbon monoxide under two-photon absorption to fine-tune its properties for use in applications.

The broadband two-photon absorption spectra of both the rhenium and manganese carbonyl

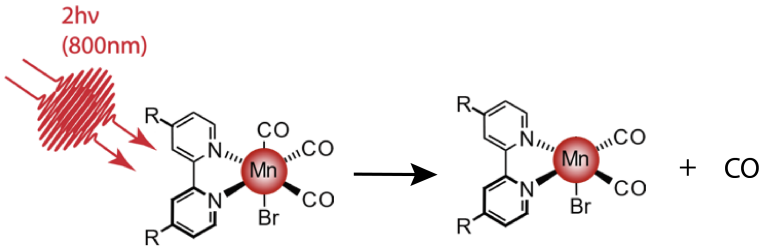

Figure 5.3: Two-photon absorption induced carbon monoxide release in manganese tricarbonyl complexes

complexes are shown in figure 5.4. In addition, the one-photon absorption spectra are overlaid for comparison of the allowed electronic transitions. The two-photon absorption spectra are complicated by the presence of stimulated Raman scattering signal from the metal complexes since the following spectra have already had the solvent contributions to the two-photon absorption and stimulated Raman scattering removed. For the rhenium complexes, the two-photon absorption spectrum matches the corresponding one-photon absorption spectrum meaning that for either excitation the molecule is reaching similar excited states. The compelling case shown in figure 5.4 is for the manganese complex the one-photon and two-photon absorption spectra are different, suggesting the possibility of different strength electronic transitions in the manganese 1PA and 2PA spectra. The measured metal to ligand charge transfer bands in the one-photon absorption spectrum had different absolute amplitudes meaning that in the case of two-photon absorption, the stronger electronic transition is located to the blue side around 330 nm instead of in the one-photon absorption case that is strongest around 410 nm.

The usefulness of broadband two-photon absorption spectroscopy to the further development of manganese tricarbonyl complexes is imperative for maximizing the two-photon absorption cross-section and understanding the photo-release of carbon monoxide under two-photon absorption. The next steps going forward to improve the usefulness of the manganese tricarbonyl for applications in photodynamic therapy is to increase the absolute two-photon absorption cross-section, maintain the ability of the photo-induced carbon monoxide, and finally work to obtain water sol-

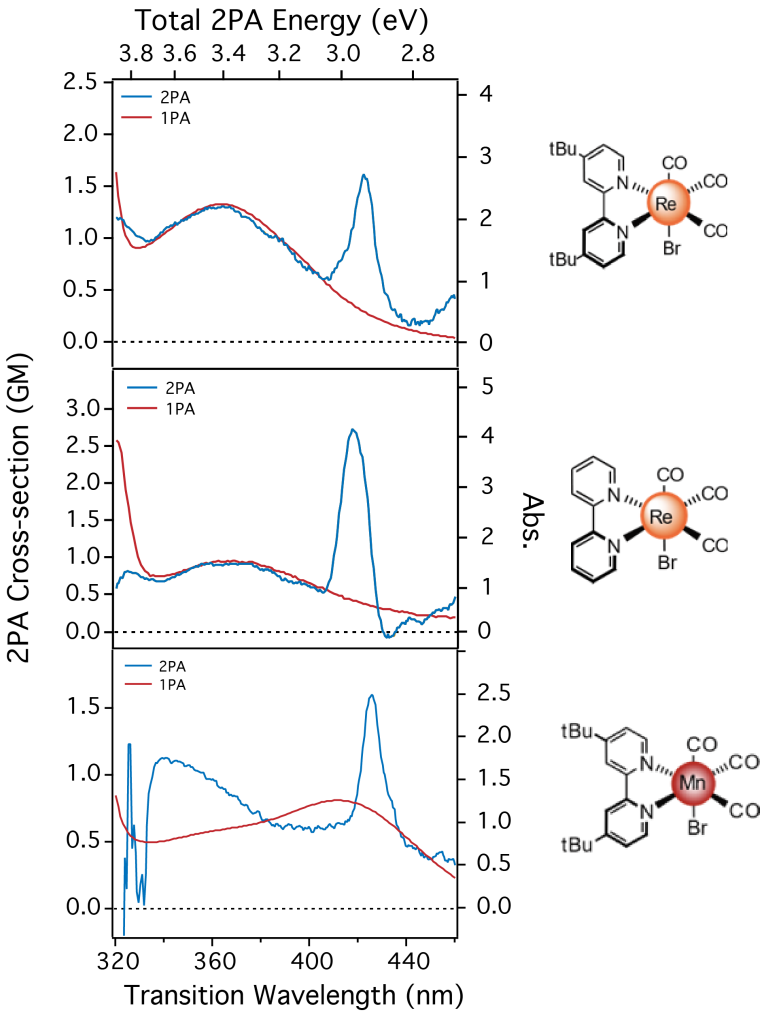

Figure 5.4: Two-photon absorption spectra of metal tricarbonyl complexes.

ubility through different derivatives of the bipyridine ligand scaffold. In order to make these improvements to the manganese tricarbonyl complexes accuarate two-photon absorption spectroscopy is needed.

The method development of the broadband 2PA technique was motivated by the many applications that take advantage of non-linear absorption that are mentioned previously. The continued development of these applications requires not only the development of new molecules with large two-photon absorption cross-sections, but also the understanding of the electronic structure and the states being reached under non-linear excitation. The ability to maximize the absolute two-photon absorption cross-section and the efficiency at which specific chemical reactions occur under non-

linear excitation requires accurate two-photon absorption spectroscopic methods. The study of the photo-active manganese metal complexes that release carbon monoxide under optical excitation was carried out to demonstrate the necessity of having broadband two-photon absorption spectra when developing and maximizing the two-photon properties for interesting applications like photodynamic therapy in the case of the carbon monoxide releasing molecules. In order to achieve a possible manganese complex that is a possible target for photodynamic therapy, a large two-photon absorption cross-section, efficient photochemical release, and solubility in water must be achieved. All these properties require an understanding of the electronic structure and the states involved with nonlinear excitation.

References

[1] Myung Kim, H., and Rae Cho, B. (2009) Two-photon materials with large two-photon cross sections. Structure-property relationship. *Chemical Communications* 153–164.

[2] Pawlicki, M., Collins, H. A., Denning, R. G., and Anderson, H. L. (2009) Two-photon absorption and the design of two-photon dyes. *Angewandte Chemie - International Edition 48*, 3244–3266.

[3] Denk, W., Strickler, J., and Webb, W. (1990) Two-photon laser scanning fluorescence microscopy. *Science 248*, 73–76.

[4] Denk, W., and Svoboda, K. (1997) Photon upmanship: Why multiphoton imaging is more than a gimmick. *Neuron 18*, 351–357.

[5] Oheim, M., Michael, D. J., Geisbauer, M., Madsen, D., and Chow, R. H. (2006) Principles of two-photon excitation fluorescence microscopy and other nonlinear imaging approaches. *Advanced Drug Delivery Reviews 58*, 788–808.

[6] Helmchen, F., and Denk, W. (2005) Deep tissue two-photon microscopy. *Nature Methods 2*, 932–940.

[7] Truong, T. V., Supatto, W., Koos, D. S., Choi, J. M., and Fraser, S. E. (2011) Deep and fast live imaging with two-photon scanned light-sheet microscopy. *Nature Methods 8*, 757–762.

[8] So, P. T. C., Dong, C. Y., Masters, B. R., and Berland, K. M. (2000) Two-Photon Excitation Fluorescence Microscopy. *Annual Review of Biomedical Engineering 2*, 399–429.

[9] Zhao, M., Zhang, H., Li, Y., Ashok, A., Liang, R., Zhou, W., and Peng, L. (2014) Cellular

imaging of deep organ using two-photon Bessel light-sheet nonlinear structured illumination microscopy. *Biomedical Optics Express 5*, 1296.

[10] Zipfel, W. R., Williams, R. M., and Webb, W. W. (2003) Nonlinear magic: multiphoton microscopy in the biosciences. *Nature Biotechnology 21*, 1369–1377.

[11] Kim, H. M., and Cho, B. R. (2015) Small-Molecule Two-Photon Probes for Bioimaging Applications. *Chemical Reviews 115*, 5014–5055.

[12] Unruh, J. R., Price, E. S., Molla, R. G., Stehno-Bittel, L., Johnson, C. K., and Hui, R. (2006) Two-photon microscopy with wavelength switchable fiber laser excitation. *Optics Express 14*, 9825.

[13] Cahalan, M. D., Parker, I., Wei, S. H., and Miller, M. J. (2002) Two-photon tissue imaging: Seeing the immune system in a fresh light. *Nature Reviews Immunology 2*, 872–880.

[14] Fan, W., Huang, P., and Chen, X. (2016) Overcoming the Achilles' heel of photodynamic therapy. *Chemical Society Reviews 45*, 6488–6519.

[15] Bolze, F., Jenni, S., Sour, A., and Heitz, V. (2017) Molecular photosensitisers for two-photon photodynamic therapy. *Chemical Communications 53*, 12857–12877.

[16] McKenzie, L. K., Sazanovich, I. V., Baggaley, E., Bonneau, M., Guerchais, V., Williams, J. A., Weinstein, J. A., and Bryant, H. E. (2017) Metal Complexes for Two-Photon Photodynamic Therapy: A Cyclometallated Iridium Complex Induces Two-Photon Photosensitization of Cancer Cells under Near-IR Light. *Chemistry - A European Journal 23*, 234–238.

[17] Karotki, A., Khurana, M., Lepock, J. R., and Wilson, B. C. (2006) Simultaneous two-photon excitation of photofrin in relation to photodynamic therapy. *Photochemistry and photobiology 82*, 443–52.

[18] Castano, A. P., Demidova, T. N., and Hamblin, M. R. (2005) Mechanisms in photodynamic therapy: Part two - Cellular signaling, cell metabolism and modes of cell death. *Photodiagnosis and Photodynamic Therapy 2*, 1–23.

[19] Heinemann, F., Karges, J., and Gasser, G. (2017) Critical Overview of the Use of Ru(II) Polypyridyl Complexes as Photosensitizers in One-Photon and Two-Photon Photodynamic Therapy. *Accounts of Chemical Research 50*, 2727–2736.

[20] Chen, Y., Guan, R., Zhang, C., Huang, J., Ji, L., and Chao, H. (2016) Two-photon luminescent metal complexes for bioimaging and cancer phototherapy. *Coordination Chemistry Reviews 310*, 16–40.

[21] Lan, M., Zhao, S., Xie, Y., Zhao, J., Guo, L., Niu, G., Li, Y., Sun, H., Zhang, H., Liu, W., Zhang, J., Wang, P., and Zhang, W. (2017) Water-Soluble Polythiophene for Two-Photon Excitation Fluorescence Imaging and Photodynamic Therapy of Cancer. *ACS Applied Materials and Interfaces 9*, 14590–14595.

[22] Boreham, E. M., Jones, L., Swinburne, A. N., Blanchard-Desce, M., Hugues, V., Terryn, C., Miomandre, F., Lemercier, G., and Natrajan, L. S. (2015) A cyclometallated fluorenyl Ir(iii) complex as a potential sensitiser for two-photon excited photodynamic therapy (2PE-PDT). *Dalton Transactions 44*, 16127–16135.

[23] Boca, S. C., Four, M., Bonne, A., Van Der Sanden, B., Astilean, S., Baldeck, P. L., and Lemercier, G. (2009) An ethylene-glycol decorated ruthenium(ii) complex for two-photon photodynamic therapy. *Chemical Communications* 4590–4592.

[24] Huang, H., Yu, B., Zhang, P., Huang, J., Chen, Y., Gasser, G., Ji, L., and Chao, H. (2015) Highly Charged Ruthenium(II) Polypyridyl Complexes as Lysosome-Localized Photosensitizers for Two-Photon Photodynamic Therapy. *Angewandte Chemie - International Edition 54*, 14049–14052.

[25] Arnbjerg, J., Jiménez-Banzo, A., Paterson, M. J., Nonell, S., Borrell, J. I., Christiansen, O., and Ogilby, P. R. (2007) Two-photon absorption in tetraphenylporphycenes: Are porphycenes better candidates than porphyrins for providing optimal optical properties for two-photon photodynamic therapy? *Journal of the American Chemical Society 129*, 5188–5199.

[26] Balaz, M., Collins, H. A., Dahlstedt, E., and Anderson, H. L. (2009) Synthesis of hydrophilic conjugated porphyrin dimers for one-photon and two-photon photodynamic therapy at NIR wavelengths. *Organic and Biomolecular Chemistry 7*, 874–888.

[27] Houk, A. L., Givens, R. S., and Elles, C. G. (2016) Two-Photon Activation of p - Hydroxyphenacyl Phototriggers : Toward Spatially Controlled Release of Diethyl Phosphate and ATP. *Journal of Physical Chemistry B 120*, 3178–3186.

[28] Hayat, A., Nevet, A., Ginzburg, P., and Orenstein, M. (2011) Applications of two-photon processes in semiconductor photonic devices: Invited review. *Semiconductor Science and Technology 26*.

[29] Rumi, M., and Perry, J. W. (2010) Two-photon absorption: an overview of measurements and principles. *Advances in Optics and Photonics 2*, 451.

[30] Harris, D. C., and Bertolucci, M. D. *Symmetry and Spectroscopy An Introduction to Vibrational and Electronic Spectroscopy*; Oxford University Press Inc., 1978; pp 330–343.

[31] McClain, W. M. (1974) Two-Photon Molecular Spectroscopy. *Accounts of Chemical Research 7*, 129–135.

[32] McClain, W. M. (1971) Excited State Symmetry Assignment Through Polarized Two-Photon Absorption Studies of Fluids. *The Journal of Chemical Physics 55*, 2789–2796.

[33] Larson, E. J., Friesen, L. A., and Johnson, C. K. (1997) An ultrafast one-photon and two-photon transient absorption study of the solvent-dependent photophysics in all-trans retinal. *Chemical Physics Letters 265*, 161–168.

[34] Ward, C. L., and Elles, C. G. (2012) Controlling the excited-state reaction dynamics of a photochromic molecular switch with sequential two-photon excitation. *Journal of Physical Chemistry Letters 3*, 2995–3000.

[35] Ward, C. L. Controlling the Cycloreversion Reaction of a Diarylethene Derivative Using Sequential Two-Photon Excitation. Ph.D. thesis, 2014.

[36] Houk, A. L., Zheldakov, I. L., Tommey, T. A., and Elles, C. G. (2015) Two-Photon Excitation of trans-Stilbene: Spectroscopy and Dynamics of Electronically Excited States above S1. *Journal of Physical Chemistry B 119*, 9335–9344.

[37] Carriles, R., Schafer, D. N., Sheetz, K. E., Field, J. J., Cisek, R., Barzda, V., Sylvester, A. W., and Squier, J. A. (2009) Invited Review Article: Imaging techniques for harmonic and multiphoton absorption fluorescence microscopy. *Review of Scientific Instruments 80*.

[38] Masanta, G., Lim, C. S., Kim, H. J., Han, J. H., Kim, H. M., and Cho, B. R. (2011) A mitochondrial-targeted two-photon probe for zinc ion. *Journal of the American Chemical Society 133*, 5698–5700.

[39] Yao, S., and Belfield, K. D. (2012) Two-photon fluorescent probes for bioimaging. *European Journal of Organic Chemistry* 3199–3217.

[40] Sarkar, A. R., Kang, D. E., Kim, H. M., and Cho, B. R. (2014) Two-photon fluorescent probes for metal ions in live tissues. *Inorganic Chemistry 53*, 1794–1803.

[41] Zhang, P., Huang, H., Chen, Y., Wang, J., Ji, L., and Chao, H. (2015) Ruthenium(II) anthraquinone complexes as two-photon luminescent probes for cycling hypoxia imaging invivo. *Biomaterials 53*, 522–531.

[42] Göstl, R., Senf, A., and Hecht, S. (2014) Remote-controlling chemical reactions by light: Towards chemistry with high spatio-temporal resolution. *Chemical Society Reviews 43*, 1982–1996.

[43] Sotome, H., Nagasaka, T., Une, K., Okui, C., Ishibashi, Y., Kamada, K., Kobatake, S., Irie, M., and Miyasaka, H. (2017) Efficient Cycloreversion Reaction of a Diarylethene Derivative in Higher Excited States Attained by Off-Resonant Simultaneous Two-Photon Absorption. *Journal of Physical Chemistry Letters 8*, 3272–3276.

[44] Michael, K. (1950) Characterization of electronic transitions in complex molecules. *Discussions of the Faraday Society* 14.

[45] Hess, J., Huang, H., Kaiser, A., Pierroz, V., Blacque, O., Chao, H., and Gasser, G. (2017) Evaluation of the Medicinal Potential of Two Ruthenium(II) Polypyridine Complexes as One- and Two-Photon Photodynamic Therapy Photosensitizers. *Chemistry - A European Journal 23*, 9888–9896.

[46] Frederiksen, P. K., McIlroy, S. P., Nielsen, C. B., Nikolajsen, L., Skovsen, E., Jørgensen, M., Mikkelsen, K. V., and Ogilby, P. R. (2005) Two-photon photosensitized production of singlet oxygen in water. *Journal of the American Chemical Society 127*, 255–269.

[47] Chen, Y., Guan, R., Zhang, C., Huang, J., Ji, L., and Chao, H. (2016) Two-photon luminescent metal complexes for bioimaging and cancer phototherapy. *Coordination Chemistry Reviews 310*, 16–40.

[48] Chapple, P., Staromlynsk, J., A., H. J., J., M. T., and McDuff R. G., (1997) Single-Beam Z-Scan: Measurement Techniques and Analysis. *Journal of Nonlinear Optical Physics and Materials 6*, 251–293.

[49] Yin, M., Li, H., Tang, S., and Ji, W. (2002) Determination of nonlinear absorption and refraction by single Z-scan method. *Applied Physics B: Lasers and Optics 70*, 587–591.

[50] Wang, Y., Wang, Y., Wang, G., and Liu, D. (2018) Two-photon absorption cross-section results of three tri-branched derivatives: A comparison between open-aperture Z-scan and two-photon excited fluorescence method. *Optik 172*, 186–190.

[51] Balu, M., Hales, J., Hagan, D. J., and Van Stryland, E. W. (2004) White-light continuum Z-scan technique for nonlinear materials characterization. *Opt. Express 12*, 3820–3826.

[52] De Boni, L., Andrade, A. A., Misoguti, L., Mendonca, C. R., and Zilio, S. C. (2004) Z-scan measurements using femtosecond continuum generation. *Optics Express 12*, 3921.

[53] Xu, C., and Webb, W. W. (1996) Measurement of two-photon excitation cross sections of molecular fluorophores with data from 690 to 1050 nm. *Journal of the Optical Society of America B 13*, 481.

[54] de Reguardati, S., Pahapill, J., Mikhailov, A., Stepanenko, Y., and Rebane, A. (2016) High-accuracy reference standards for two-photon absorption in the 680–1050 nm wavelength range. *Optics Express 24*, 9053.

[55] Makarov, N. S., Drobizhev, M., and Rebane, A. (2008) Two-photon absorption standards in the 550-1600 nm excitation wavelength range. *16*, 4029–4047.

[56] Hales, J. M., Belfield, K. D., Balu, M., Schafer, K. J., Hagan, D. J., and Van Stryland, E. W. (2003) Two-photon absorption cross-sections of common photoinitiators. *Journal of Photochemistry and Photobiology A: Chemistry 162*, 497–502.

[57] Xu, C., and Webb, W. W. (1995) Measurement of two-photon excitation cross sections of molecular fluorophores with data from 690 to 1050 nm. *Journal of the Optical Society of America B 13*, 481.

[58] Negres, R. A., Hales, J. M., Kobyakov, A., Hagan, D. J., and Van Stryland, E. W. (2002) Experiment and analysis of two-photon absorption spectroscopy using a white-light continuum probe. *IEEE Journal of Quantum Electronics 38*, 1205–1216.

[59] Negres, R. a., Hales, J. M., Kobyakov, A., Hagan, D. J., and Van Stryland, E. W. (2002) Two-photon spectroscopy and analysis with a white-light continuum probe. *Optics letters 27*, 270–272.

[60] Elles, C. G., Rivera, C. A., Zhang, Y., Pieniazek, P. A., and Bradforth, S. E. (2009) Electronic structure of liquid water from polarization-dependent two-photon absorption spectroscopy. *Journal of Chemical Physics 130*.

[61] Bhattacharyya, D., Zhang, Y., Elles, C. G., and Bradforth, S. E. (2019) Electronic Structure of Liquid Methanol and Ethanol from Polarization-Dependent Two-Photon Absorption Spectroscopy. *Journal of Physical Chemistry A 123*, 5789–5804.

[62] Hosoi, H., Tayama, R., Takeuchi, S., and Tahara, T. (2015) Solvent dependence of two-photon absorption spectra of the enhanced green fluorescent protein (eGFP) chromophore. *Chemical Physics Letters 630*, 32–36.

[63] Trebino, R., and Kane, D. J. (1993) Using phase retrieval to measure the intensity and phase of ultrashort pulses: frequency-resolved optical gating. *Journal of the Optical Society of America 10*, 1101–1111.

[64] Trebino, R., DeLong, K. K. W., Fittinghoff, D. N. D., Sweetser, J. N. J., Krumbugel, M., Richman, B. a. B., and Kane, D. J. D. (1997) Measuring ultrashort laser pulses in the time-frequency domain using frequency-resolved optical gating. *Review of Scientific Instruments 68*, 3277.

[65] McCamant, D. W., Kukura, P., Yoon, S., and Mathies, R. A. (2004) Femtosecond broadband stimulated Raman spectroscopy: Apparatus and methods. *Review of Scientific Instruments 75*, 4971–4980.

[66] Quincy, T. J. Direct and Indirect Probing of Higher-Lying Excited-States of Photoactive Molecules. Ph.D. thesis, 2018.

[67] Pontecorvo, E., Ferrante, C., Elles, C. G., and Scopigno, T. (2013) Spectrally tailored narrowband pulses for femtosecond stimulated Raman spectroscopy in the range 330-750 nm. *Optics Express 21*, 6866.

[68] Kaiser, W., and Garrett, C. G. B. (1961) Physical review letters of two-photon excitation in CaF Eu'+. *Physical Review 7*, 229–231.

[69] Bridges, R. E., Fischer, G. L., and Boyd, R. W. (1995) Z-scan measurement technique for non-Gaussian beams and arbitrary sample thicknesses. *Optics Letters 20*, 1821.

[70] Sheik-Bahae, M., Said, A. A., Wei, T.-h., Hagan, D. J., and Van Stryland, E. W. (1990) Sensitive measurement of optical nonlinearities using a single beam - Quantum Electronics, IEEE Journal of. *Quantum Electronics 26*, 760–769.

[71] Hermann, J. P., and Ducuing, J. (1972) Absolute measurement of two-photon cross sections. *Physical Review A 5*, 2557–2568.

[72] Balu, M., Hales, J., Hagan, D. J., and Van Stryland, E. W. (2004) White-light continuum Z-scan technique for nonlinear materials characterization. *Opt. Express 12*, 3820–3826.

[73] He, G., Lin, T.-C., Prasad, P., Kannan, R., Vaia, R., and Tan, L.-S. (2002) New technique for degenerate two-photon absorption spectral measurements using femtosecond continuum generation. *Optics Express 10*, 566.

[74] Bewersdorf, J., Allgeyer, E. S., Grutzendler, J., Yuan, P., and Velasco, M. G. M. (2015) Absolute two-photon excitation spectra of red and far-red fluorescent probes. *Optics Letters 40*, 4915.

[75] Isobe, K., Kawano, H., Suda, A., Kumagai, A., Miyawaki, A., and Midorikawa, K. (2013) Simultaneous imaging of two-photon absorption and stimulated Raman scattering by spatial overlap modulation nonlinear optical microscopy. *Biomedical Optics Express 4*, 1548.

[76] Elles, C. G., Rivera, C. A., Zhang, Y., Pieniazek, P. A., and Bradforth, S. E. (2009) Electronic structure of liquid water from polarization-dependent two-photon absorption spectroscopy. *Journal of Chemical Physics 130*.

[77] Prince, R. C., Frontiera, R. R., and Potma, E. O. (2017) Stimulated Raman scattering: From bulk to nano. *Chemical Reviews 117*, 5070–5094.

[78] Yamaguchi, S., and Tahara, T. (2003) Two-photon absorption spectrum of all-trans retinal. *Chemical Physics Letters 376*, 237–243.

[79] Ekvall, K., van der Meulen, P., Dhollande, C., Berg, L.-E., Pommeret, S., Naskrecki, R., and Mialocq, J.-C. (2000) Cross phase modulation artifact in liquid phase transient absorption spectroscopy. *Journal of Applied Physics 87*, 2340–2352.

[80] Kovalenko, S. A., Dobryakov, A. L., Ruthmann, J., and Ernsting, N. P. (1999) Femtosecond spectroscopy of condensed phases with chirped supercontinuum probing. *Physical Review A - Atomic, Molecular, and Optical Physics 59*, 2369–2384.

[81] Griffiths, J. E. (1974) Raman scattering cross sections in strongly interacting liquid. *Journal of Chemical Physics 2556*, 5–7.

[82] Friedrich, D. M., and McClain, W. M. (1980) Two-Photon Molecular Electronic Spectroscopy. *Annual Review of Physical Chemistry 31*, 559–577.

[83] Thomas, J. K. (2014) Higher excited states in multiphoton photochemical reactions "hint" toward rapid chemistry. *Journal of Physical Chemistry Letters 5*, 2586–2587.

[84] Long, D. A. *Structural Chemistry*; 2002; Vol. 8; p 611.

[85] Shim, S., and Mathies, R. A. (2006) Generation of narrow-bandwidth picosecond visible pulses from broadband femtosecond pulses for femtosecond stimulated Raman. *Applied Physics Letters 89*, 2004–2007.

[86] Luo, H., Qian, L., Yuan, P., and Zhu, H. (2006) Generation of tunable narrowband pulses initiating from a femtosecond optical parametric amplifier. *Optics Express 14*, 10631.

[87] Marangoni, M., Brida, D., Quintavalle, M., Cirmi, G., Pigozzo, F. M., Manzoni, C., Baronio, F., Capobianco, A. D., and Cerullo, G. (2007) Narrow-bandwidth picosecond pulses

by spectral compression of femtosecond pulses in a second- order nonlinear crystal. *Optics Express 15*, 174–180.

[88] Sponer, H., Nordheim, G., Sklar, A. L., and Teller, E. (1939) Analysis of the near ultraviolet electronic transition of benzene. *The Journal of Chemical Physics 7*, 207–220.

[89] Broude, V. (1961) Spectroscopic studies of benzene. *Soviet Physics Uspekhi 4*, 584–608.

[90] Hochstrasser, R. M., Sung, H. N., and Wessel, J. E. (1973) Two-Photon Excitation Spectra. A New and Versatile Spectroscopic Tool. *Journal of the American Chemical Society 95*, 8179–8180.

[91] Wunsch, L., Metz, F., Neusser, H. J., and Schlag, E. W. (1977) Two-photon spectroscopy in the gas phase: Assignments of molecular transitions in benzene. *The Journal of Chemical Physics 66*, 386–400.

[92] Lombardi, J. R., Wallenstein, R., Hänsch, T. W., and Friedrich, D. M. (1976) High resolution two-photon spectroscopy in the1B2ustate of benzene. *The Journal of Chemical Physics 65*, 2357–2366.

[93] Wunsch, L., Neusser, H. J., and Schlag, E. W. (1974) Two Photon Excitation Spectrum of Benzene d6 In The Gas Phase: Assignment of Inducing Modes byHot Band Analysis. *31*, 433–439.

[94] Hochstrasser, R. M., Wessel, J. E., and Sung, H. N. (1974) Two-photon excitation spectrum of benzene in the gas phase and the crystal. *Journal of Chemical Physics 60*, 317–318.

[95] Hochstrasser, R. M., Klimcak, C. M., and Meredith, G. R. (1979) Vibronic spectra of the benzene crystal at 4.2 K using two-photon fluorescence excitation. *The Journal of Chemical Physics 70*, 870–880.

[96] Rice, J. K., and Anderson, R. W. (1986) Two-photon, thermal lensing spectroscopy of mono-substituted benzenes. *The Journal of Physical Chemistry 90*, 6793–6800.

[97] Fernández-Sánchez, J. M., and Montero, S. (1989) Gas phase Raman scattering cross sections of benzene and perdeuterated benzene. *The Journal of Chemical Physics 90*, 2909–2914.

[98] Schomacker, K. T., Delaney, J. K., and Champion, P. M. (1986) Measurements of the absolute Raman cross sections of benzene. *The Journal of Chemical Physics 85*, 4240–4247.

[99] Lawson, C. W., Hirayama, F., and Lipsky, S. (1969) Effect of solvent perturbation on the S2 S1 internal conversion efficiency of benzene,toluene, and-p-xylene. *The Journal of Chemical Physics 51*, 1590–1596.

[100] Strommen, D. P. (2009) Specific values of the depolarization ratio in Raman spectroscopy: Their origins and significance. *Journal of Chemical Education 69*, 803.

[101] Proffitt, W., and Porto, S. P. S. (1973) Depolarization ratio in Raman spectroscopy as a function of frequency. *Journal of the Optical Society of America 63*, 77.

[102] Lee, D., Akturk, S., Gabolde, P., and Trebino, R. (2007) Experimentally simple, extremely broadband transient-grating frequency-resolved-opticalgating arrangement. *Optics Express 15*, 760–766.

[103] Sweetser, J. N., Fittinghoff, D. N., and Trebino, R. (1997) Transient-grating frequency-resolved optical gating. *Optics Letters 22*, 519–521.

[104] Kane, D. J., and Trebino, R. (1993) Single-shot measurement of the intensity and phase of an arbitrary ultrashort pulse by using frequency-resolved optical gating. *Optics Letters 18*, 823.

[105] Alberto, R., and Motterlini, R. (2007) Chemistry and biological activities of CO-releasing molecules (CORMs) and transition metal complexes. *Dalton Transactions* 1651–1660.

[106] Wright, M. A., and Wright, J. A. (2016) PhotoCORMs: CO release moves into the visible. *Dalton Transactions 45*, 6801–6811.